

Remote Sensing Handbook:
Land Resources: Monitoring, Modelling, and Mapping
Volume II, Chapter 7

**Global Cropland Area Database (GCAD) derived from Remote
Sensing in Support of Food Security in the Twenty-first Century:
Current Achievements and Future Possibilities**

**Pardhasaradhi Teluguntla^{1,2}, Prasad S. Thenkabail¹, Jun Xiong^{1,3},
Murali Krishna Gumma⁴, Chandra Giri⁵, Cristina Milesi⁶, Mutlu Ozdogan⁷,
Russ Congalton⁸, James Tilton⁹, Temuulen Tsagaan Sankey³, Richard Massey³,
Aparna Phalke⁷, and Kamini Yadav⁸**

1 = U. S. Geological Survey (USGS), 2255, N. Gemini Drive, Flagstaff, AZ 86001, USA

2 = Bay Area Environmental Research Institute (BAERI), 596 1st St West Sonoma, CA 95476, USA

3 = School of Earth Sciences and Environmental Sustainability (SESES), Northern Arizona University, Flagstaff,
AZ 86011, USA

4 = International Crops Research Institute for the Semi Arid Tropics (ICRISAT), Patancheru, Hyderabad, India

5 = U. S. Geological Survey (USGS), (EROS) Center, Sioux Falls, SD, USA

6 = NASA Ames Research Center, MS 242-4, Moffett Field, CA 94035, USA

7 = University Of Wisconsin, 1710 University Avenue, Madison, WI 53726, USA

8 = University of New Hampshire, 215 James Hall, 56 College Road, Durham, NH 03824, USA

9 = NASA Goddard Space Flight Center (GSFC), Greenbelt, MD 20771, USA

Email: pteluguntla@usgs.gov, pthenkabail@usgs.gov, jxiong@usgs.gov, m.gumma@cgiar.org ,
cristina.milesi@gmail.com, ozdogan@wisc.edu, russ.congalton@unh.edu, james.c.tilton@nasa.gov,
Temuulen.Sankey@nau.edu, rmassey@usgs.gov, phalke@wisc.edu, kaminiyadav.02@gmail.com

1.0 Introduction

2.0 Global distribution of croplands and other land use and land cover: Baseline

2.1 Existing global cropland maps: Remote sensing and non-remote sensing approaches

3.0 Key remote sensing derived cropland products: in support of global food security

4.0 Definition of cropland mapping using remote sensing

5.0 Data: Remote sensing and other data for global cropland mapping

5.1 Primary satellite sensor data

5.2 Secondary data

5.3 Field-plot Data

5.4 Very high resolution imagery data

5.5 Data composition: Mega File Data Cube (MFDC) concept

6.0 Methods of cropland mapping

6.1 Cropland mapping methods using remote sensing at global, regional, and local scales

6.1.1 Spectral Matching Techniques (SMTs) Algorithms

6.1.1.1 Spectral Matching Techniques (SMTs)

6.1.2.2 Generating Class Spectra

6.1.2.3 Ideal Spectra Data Bank on Irrigated Areas (ISDB IA)

6.2 Automated Cropland Classification Algorithm (ACCA)

7.0 Remote sensing based global cropland products: current state-of-art, their strengths, and limitations

7.1 Global cropland extent at nominal 1-km resolution

8.0 Change Analysis

9.0 Limitations of existing cropland products

10.0 Way forward

11.0 Conclusions

12.0 Acknowledgements

13.0 References

1.0 Introduction

The precise estimation of the global agricultural cropland- extents, areas, geographic locations, crop types, cropping intensities, and their watering methods (irrigated or rainfed; type of irrigation) provides a critical scientific basis for the development of water and food security policies (Thenkabail et al., 2012, 2011, 2010). By year 2100, the global human population is expected to grow to 10.4 billion under median fertility variants or higher under constant or higher fertility variants (Table 1) with over three quarters living in developing countries, in regions that already lack the capacity to produce enough food. With current agricultural practices, the increased demand for food and nutrition would require in about 2 billion hectares of additional cropland, about twice the equivalent to the land area of the United States, and lead to significant increases in greenhouse gas productions (Tillman *et al.*, 2011). For example, during 1960-2010 world population more than doubled from 3 billion to 7 billion. The nutritional demand of the population also grew swiftly during this period from an average of about 2000 calories per day per person in 1960 to nearly 3000 calories per day per person in 2010. The food demand of increased population along with increased nutritional demand during this period (1960-2010) was met by the “green revolution” which more than tripled the food production; even though croplands decreased from about 0.43 ha/capita to 0.26 ha/capita (FAO, 2009). The increase in food production during the green revolution was the result of factors such as: (a) expansion in irrigated areas which increased from 130 Mha in 1960s to 278.4 Mha in year 2000 (Siebert et al., 2006) or 399 Mha when you do not consider cropping intensity (Thenkabail et al., 2009a, 2009b, 2009c) or 467 Mha when you consider cropping intensity (Thenkabail et al., 2009a; Thenkabail et al., 2009c); (b) increase in yield and per capita food production (e.g., cereal production from 280 kg/person to 380 kg/person and meat from 22 kg/person to 34 kg/person (McIntyre, 2008); (c) new cultivar types (e.g., hybrid varieties of wheat and rice, biotechnology); and (d) modern agronomic and crop management practices (e.g., fertilizers, herbicide, pesticide applications). However, some of the factors that lead to the green revolution have stressed the environment to limits leading to salinization and decreasing water quality. For example, from 1960 to 2000, the phosphorous use doubled from 10 million tons to 20 MT, pesticide use tripled from near zero to 3 MT, and nitrogen use as fertilizer increased to a staggering 80 MT from just 10 MT (Foley et al., 2007; Khan and Hanjra, 2008). Further, diversion of croplands to bio-fuels is already taking water away from food production; the economics, carbon sequestration, environmental, and food security impacts of biofuel production are net negative (Lal and Pimentel, 2009), leaving us with a carbon debt (Gibbs et al., 2008; Searchinger et al., 2008). Climate models predict that in most regions of the world the hottest seasons on record will become the norm by the end of the century-an outcome that bodes ill for feeding the world (Kumar and Singh, 2005). Also, crop yield increases of the green revolution era have now stagnated (Hossain et al., 2005). Thereby, further increase in food production through increase in cropland areas and/or increased allocations of water for croplands are widely considered unsustainable and/or infeasible. Indeed, cropland areas have even begun to decrease in many

parts of the World due to factors such as urbanization, industrialization, and salinization. Furthermore, ecological and environmental imperatives such as biodiversity conservation and atmospheric carbon sequestration have put a cap on the possible expansion of cropland areas to other lands such as forests and rangelands. Other important factors limit food security. These include factors such as diversion of croplands to biofuels (Bindraban et al., 2009), limited water resources for irrigation expansion (Turrall et al., 2009), limits on agricultural intensifications, loss of croplands to urbanization (Khan and Hanjra, 2008), increasing meat consumption (and associated demands on land and water) (Vinnari and Tapiola, 2009), environmental infeasibility for cropland expansion (Gordon et al., 2009), and changing climate have all put pressure on our continued ability to sustain global food security in the twenty-first century. So, how does the World continue to meet its food and nutrition needs?. Solutions may come from bio-technology and precision farming, however developments in these fields are not currently moving at rates that will ensure global food security over next few decades. Further, there is a need for careful consideration of possible harmful effects of bio-technology. We should not be looking back 30–50 years from now, like we have been looking back now at many mistakes made during the green revolution. During the green revolution the focus was only on getting more yield per unit area. Little thought was put about serious damage done to our natural environments, water resources, and human health as a result of detrimental factors such as uncontrolled use of herbicides-pesticides-nutrients, drastic groundwater mining, and salinization of fertile soils due to over irrigation. Currently, there is talk of a “second green revolution” or even an “ever green revolution”, but clear ideas on what these terms actually mean are still debated and are evolving. One of the biggest issues that are not given adequate focus is the use of large quantities of water for food production. Indeed, an overwhelming proportion (60–90%) of all human water use in India goes for producing their food (Falkenmark, M., & Rockström, 2006). But such intensive water use for food production is no longer tenable due to increasing pressure for water use alternatives such as increasing urbanization, industrialization, environmental flows, bio-fuels, and recreation. This has brought into sharp focus the need to grow more food per drop of water leading to a “blue revolution”.

Table 1. World population (thousands) under all variants, 1950–2100.

Year	Medium fertility variant	High fertility variant	Low fertility variant	Constant fertility variant
1950	2,529,346	2,529,346	2,529,346	2,529,346
1955	2,763,453	2,763,453	2,763,453	2,763,453
1960	3,023,358	3,023,358	3,023,358	3,023,358
1965	3,331,670	3,331,670	3,331,670	3,331,670
1970	3,685,777	3,685,777	3,685,777	3,685,777
1975	4,061,317	4,061,317	4,061,317	4,061,317
1980	4,437,609	4,437,609	4,437,609	4,437,609
1985	4,846,247	4,846,247	4,846,247	4,846,247
1990	5,290,452	5,290,452	5,290,452	5,290,452

1995	5,713,073	5,713,073	5,713,073	5,713,073
2000	6,115,367	6,115,367	6,115,367	6,115,367
2005	6,512,276	6,512,276	6,512,276	6,512,276
2010	6,916,183	6,916,183	6,916,183	6,916,183
2015	7,324,782	7,392,233	7,256,925	7,353,522
2020	7,716,749	7,893,904	7,539,163	7,809,497
2025	8,083,413	8,398,226	7,768,450	8,273,410
2030	8,424,937	8,881,519	7,969,407	8,750,296
2035	8,743,447	9,359,400	8,135,087	9,255,828
2040	9,038,687	9,847,909	8,255,351	9,806,383
2045	9,308,438	10,352,435	8,323,978	10,413,537
2050	9,550,945	10,868,444	8,341,706	11,089,178
2055	9,766,475	11,388,551	8,314,597	11,852,474
2060	9,957,399	11,911,465	8,248,967	12,729,809
2065	10,127,007	12,442,757	8,149,085	13,752,494
2070	10,277,339	12,989,484	8,016,514	14,953,882
2075	10,305,146	13,101,094	7,986,122	15,218,723
2080	10,332,223	13,213,515	7,954,481	15,492,520
2085	10,358,578	13,326,745	7,921,618	15,775,624
2090	10,384,216	13,440,773	7,887,560	16,068,398
2095	10,409,149	13,555,593	7,852,342	16,371,225
2100	10,433,385	13,671,202	7,815,996	16,684,501

Source: UNDP (2012).

A significant part of the solution lies in developing an advanced global cropland area database (GCAD) with an ability to map global croplands and their attributes routinely, rapidly, consistently, and with sufficient accuracies. This, in turn, will help us determine how global croplands are used and how they might be better managed to optimize use of resources in food production. Given the complexities of global croplands (Thenkabail et al., 2012, 2010), remote sensing will play an increasingly critical role in supporting data collection and policy formation. This will include the creation of a framework of best practices and an advanced global geospatial information system on global croplands. Such a system would need to be consistent across nations and regions by providing information on issues such as the composition and location of cropping, cropping intensities (e.g. single, double crop), rotations, crop health/vigor, irrigation status. Opportunities to establish such a global system can be achieved by fusing advanced remote sensing data from multiple platforms and agencies (e.g., http://eros.usgs.gov/ceos/satellites_midres1.shtml; <http://www.ceos-cove.org/index.php>) in combination with national statistics, secondary data (e.g., elevation, slope, soils, temperature, precipitation), and the systematic collection of field level observations. The GCAD will be a major contribution to Group on Earth Observations (GEO) Global Agricultural Monitoring Initiative (GLAM), to the overarching vision of GEO Agriculture and Water Societal Beneficial

Areas (GEO Ag. SBAs), G20 Agriculture Ministers initiatives, and ultimately to the Global Earth Observation System of Systems (GEOSS). These initiatives are also supported by the Committee on Earth Observing Satellites (CEOS) Strategic Implementation Team (SIT).

Given the above facts, the overarching goal of this chapter is to provide a comprehensive overview of the state-of-art of global cropland mapping using remote sensing. First, the chapter will provide an overview of existing cropland maps and their characteristics along with establishing the gap in knowledge in global cropland mapping. Second, definitions of cropland mapping along with key parameters involved in cropland mapping based on their importance in food security analysis, and cropland naming conventions for standardized cropland mapping using remote sensing will be presented. Third, existing methods and approaches of cropland mapping will be discussed. This will include the type of remote sensing data used in cropland mapping and their characteristics along with discussions on the secondary data, field-plot data, and cropland mapping algorithms (CMAs). Fourth, currently existing global cropland products derived using remote sensing will be presented and discussed. Fifth, a synthesis of all existing products leading to a composite global cropland extent version 1.0 (GCE V1.0) is presented and discussed. Sixth, a way forward for advanced global cropland mapping is visualized.

2.0 Global distribution of croplands and other land use and land cover: Baseline

Spatial distribution of global croplands along with other land use and land cover classes is shown in Figure 1. Class 8 and 9 (Figure 1) have zero croplands that occupy 44% (~4200 Landsat scenes out of 9550) of the total terrestrial land. Further, class 6 with 17% terrestrial area is forests, class 7 with 12% terrestrial area is deserts. In these areas <5% of the total croplands exist. So, in order to study croplands systematically and intensely, prioritize areas of classes 1 to 5 (26% of the terrestrial area) where 95% of all global croplands exists with first 3 classes (class 1, 2, 3) having ~75% and the next 3 ~20% (Figure 1). Figure 1 provides a first view of where global croplands are and help us focus on these geographic locations for detailed cropland studied. In the future, it is likely some of the non-croplands may be converted to croplands or vice versa. Segmenting the world into distinct cropland versus non-cropland areas will help us understand and study these change dynamics better.

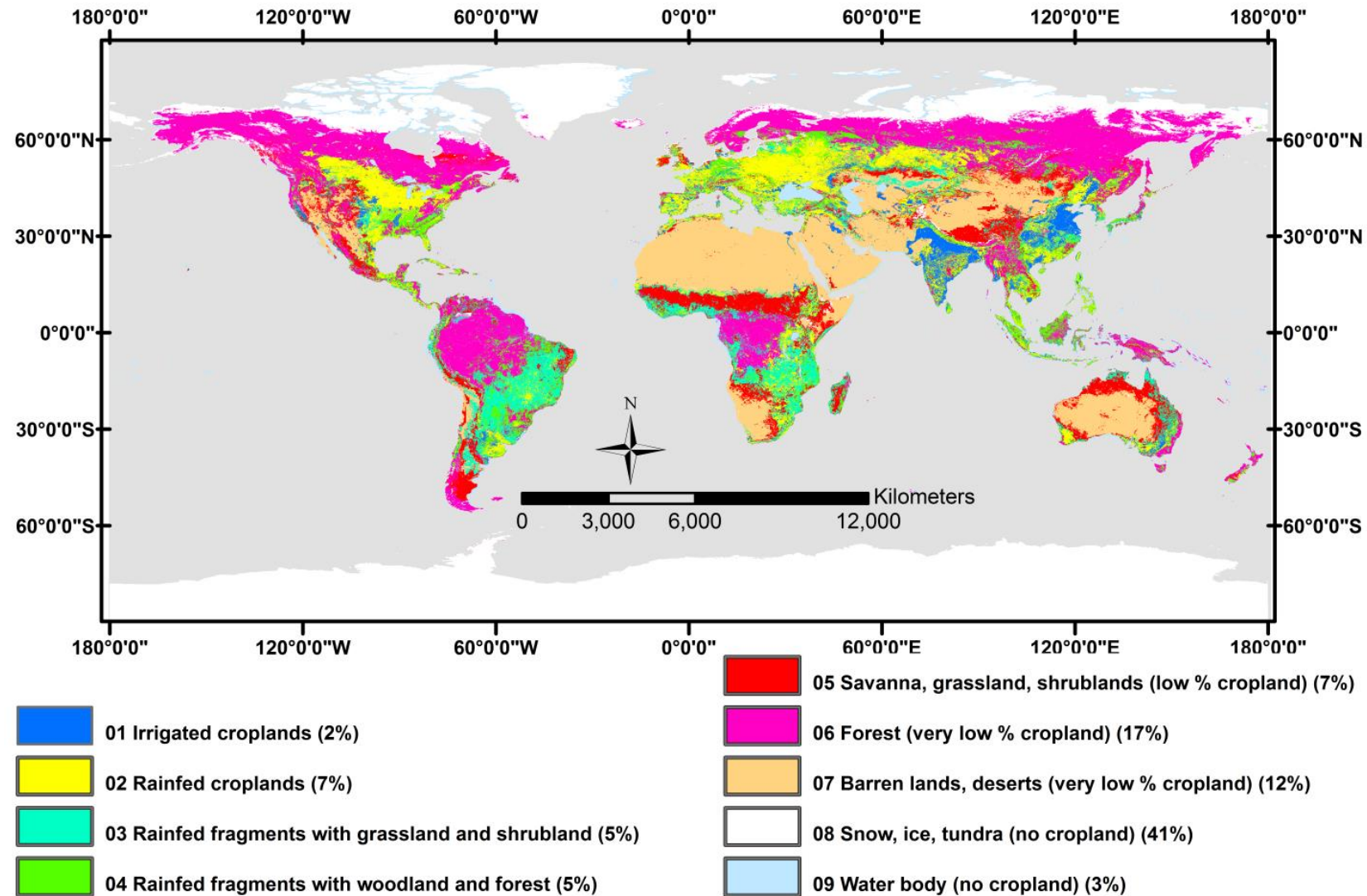


Figure 1. Global croplands and other land use and land cover: Baseline.

2.1 Existing global cropland maps: Remote sensing and non-remote sensing approaches

There are currently six major global cropland maps: (1) Thenkabail et al. (2009a,b), (2) Ramankutty et al. (1998), (3) Goldewijk et al. (2011), (4) Portmann et al. (2009) and Siebert and Döll (2009); (5) Pittman et al. (2010) and (6) Yu et al. (2013). These studies estimated the total global cropland area to be around 1.5 billion hectares, for the year 2000 baseline. However, there are 2 significant differences in these products: 1. spatial disagreement on where the actual croplands are, and 2. Irrigated to rainfed cropland proportions and their precise spatial locations. Globally, cropland areas have increased from around 265 Mha in year 1700 to around 1,471 Mha in year 1990, whilst the area of pasture has increased approximately six fold from 524 to 3,451 Mha (Foley et al., 2011). Ramankutty and Foley (1998) estimated the cropland and pasture to represent about 36% of the world's terrestrial surface ($148,940,000 \text{ km}^2$), of which, according to different studies, roughly 12% is croplands and 24% pasture. Multiple studies (Goldewijk et al., 2011; Portmann et al., 2008; Ramankutty et al., 2008) integrated agricultural statistics and census data from the national systems with spatial mapping technologies involving geographic information systems (GIS) to derive global cropland maps.

Thenkabail and others (2011, 2009a,b) produced the first remote sensing based global irrigated and rainfed cropland maps and statistics through multi-sensor remote sensing data fusion along with secondary data, and in-situ data. They further used 5 dominant crop types (wheat, rice, corn, barley and soybeans) produced using parcel-based inventory data (Monfreda et al., 2008; Portmann et al., 2008; Ramankutty et al., 2008) to produce global croplands with crop dominance (Thenkabail et al., 2012). The five crops account for about 60% of the total global cropland areas. The precise spatial location of these crops is only an approximation due to the coarse resolution (approx. 1 km^2) and fractional representation (1 to 100% crop in a pixel) of the crop data in each grid cell of all the maps from which this composite map is produced (Thenkabail et al. 2012). The existing global cropland datasets also differ from each other due to inherent uncertainties in establishing the precise location of croplands, the watering methods (rainfed *versus* irrigated), cropping intensities, crop types and/or dominance, and crop characteristics (e.g. crop or water productivity measures such as biomass, yield, and water use). Improving knowledge of the uncertainties (Congalton and Green, (2009)) in these estimates will lead to a suite of highly accurate spatial data products in support of crop modeling, food security analysis, and decision support.

3.0 Key remote sensing derived cropland products: in support of global food security

The key cropland information systems for global food security analysis derived using remote sensing include (Figure 2): (a) cropland extent\areas, (b) watering methods (e.g., irrigated, supplemental irrigated, rainfed), (c) crop types, and (d) cropping intensities (e.g., single crop, double crop, continuous crop). Many other parameters such as: (e) precise location of crops, (f) cropping calendar, (g) crop health\vigor, (h) flood and drought information, (i) water use assessments, and (j) yield or productivity (expressed per unit of land and\or unit of water), are also often derived but will not be focus of this chapter. Given the global nature of the cropland information system using remote sensing, we will focus on the 4 key products (Figure 2). Remote sensing is specifically suited to derive these products over large areas using fusion of advanced remote sensing (e.g., Landsat, Resourcesat, MODIS) in combination with national statistics, ancillary data (e.g., elevation, precipitation), and field-plot data. Such a system, at the global level, will be complex in data handling and processing and requires coordination between

multiple agencies leading to development of a seamless, scalable, transparent, and repeatable methodology. As a result, it is important to have systematic class labeling convention as illustrated in Figure 3. A standardized class identifying and labeling process (Figure 3) will enable consistent and systematic labeling of classes, irrespective of analysts. First, area is separated into cropland versus non-croplands. Then, within cropland class labeling will involve (Figure 3): (a) cropland extent (cropland vs. non-cropland), (b) watering source (e.g., irrigated versus rainfed), (c) irrigation source (e.g., surface water, ground water), (d) crop type or dominance, (e) scale (e.g., large or contiguous, small or fragmented), and (f) cropping intensity (e.g., single crop, double crop). The detail at which one maps at each stage and each parameter would depend on so many factors such as resolution of the imagery, available ground data, and expert knowledge. For example, if there is no sufficient knowledge on whether the irrigation is by surface water or ground water, but is clear that the area is irrigated; one could just map it as irrigated without mapping greater details on what type of irrigation. But, for every cropland class, one has the potential to map the details as shown in Figure 3.

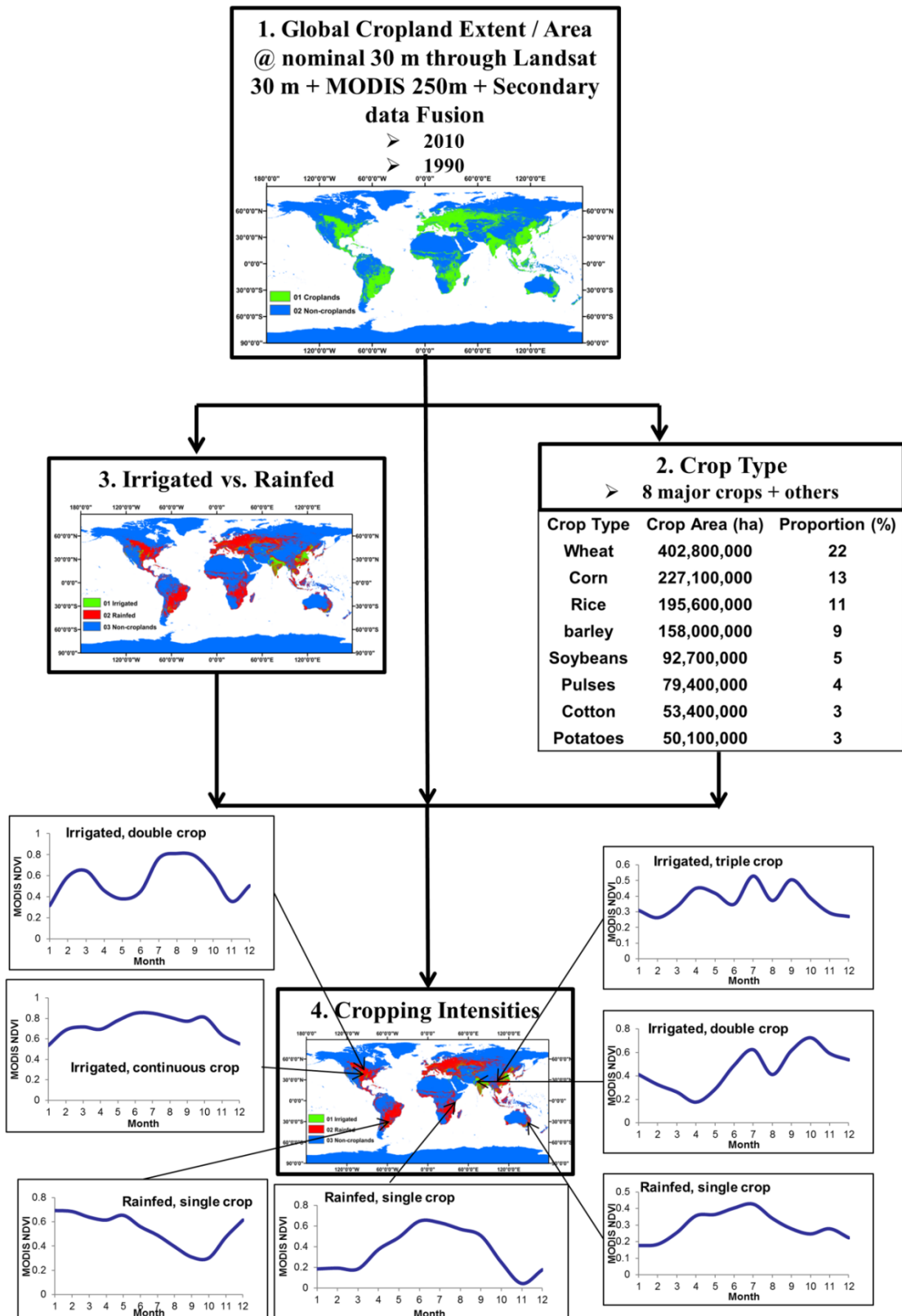
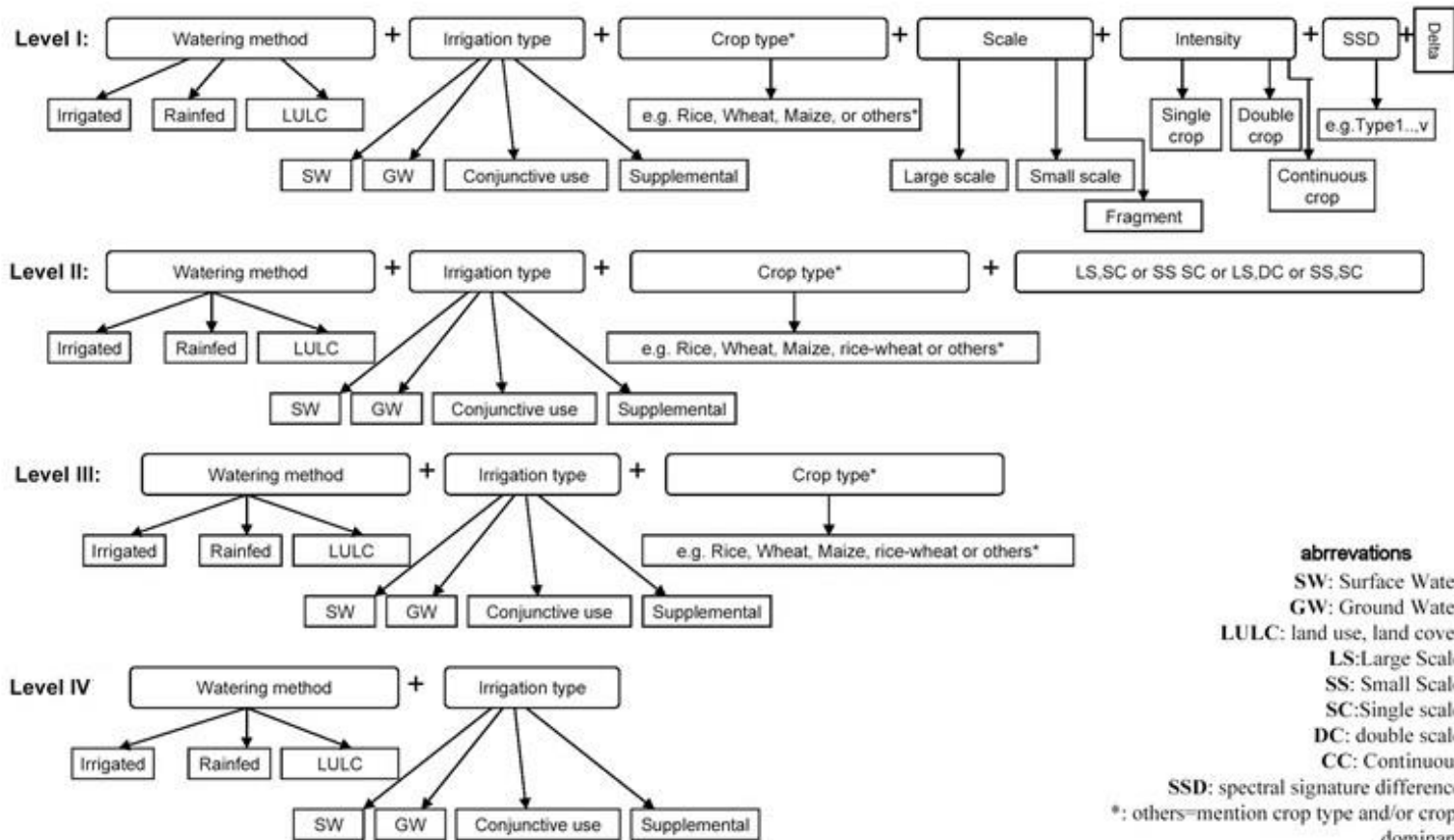


Figure 2. Key global cropland area products that will support food security analysis in the twenty-first century.



abbreviations

SW: Surface Water

GW: Ground Water

LULC: land use, land cover

LS: Large Scale

SS: Small Scale

SC: Single scale

DC: double scale

CC: Continuous

SSD: spectral signature difference

*: others=mention crop type and/or crop dominant

Figure 3. Cropland class naming convention at different levels. Level I being most detailed and level IV being least detailed.

4.0 Definition of cropland mapping using remote sensing

Key to mapping is in definitions on what we map. It is often the first and primary step. Different definitions will lead to different products. For example, irrigated areas are defined and understood differently. One can define them as areas which get irrigation at least once during their crop growing period. Alternatively they can be defined as areas which get irrigation to meet at least half their crop water requirements during the growing season. One other definition can be that these are areas that are irrigated throughout the growing season. In each of these cases the irrigated area extent mapped will vary. Similarly croplands can be defined as all agricultural areas irrespective of type of crops grown or they may be limited to food crops (and not the fodder crops or plantation crops). So, it is obvious that having a clear understanding of the definitions of what we map is extremely important for the integrity of the products developed. The “Global Food Security Support Analysis Data @ 30 m (GFSAD30)” project working group team defined cropland products as follows:

- **Minimum mapping unit**
When 3 by 3 (0.81 hectares) Landsat pixels are cropped by a same crop, then that falls into a particular crop type.
- **Cropland extent**
All cultivated plants harvested for food, feed, and fiber, including plantations (e.g., orchards, vineyards, coffee, tea, rubber).
- **What is a cropland pixel?**
>50% of pixel is cropped
- **Irrigated areas:** artificial application of any amount of water to overcome crop water stress. Irrigated areas are those areas which are irrigated one or more times during crop growing season
- **Rainfed areas:** areas that have no irrigation whatsoever and are precipitation dependent.
- **Cropping intensity**
Number of cropping cycles within a 12 month period
- **Crop type**
8 crops (Wheat, Corn, Rice, Barley, Soybeans, Pulses, Cotton, Potatoes)

Others: However, the cropland products discussed in this chapter all have different definitions as we will see in section 3.0 and its sub sections.

5.0 Data: Remote sensing and other data for global cropland mapping

Cropland mapping using remote sensing involves multiple types of data: satellite sensor data, secondary data, statistical data, and field plot data. When these data are used in an integrated fashion, the output products achieve highest possible accuracies.

5.1 Primary satellite sensor data

Cropland mapping will require satellite sensor data across spatial, spectral, radiometric, and temporal resolutions from wide array of satellite/sensor platforms (Table 2) throughout the growing season. These satellites and sensors are “representative” at hyperspectral, multispectral, and hyperspatial data. The data points per hectare (Table 2, last column) will tell us the spatial detail of agricultural information gathered. In addition to satellite based sensors, it is always valuable to gather ground based hand-held spectroradiometer data from hyperspectral sensors and\or imaging spectroscopy from ground based, airborne, or space borne sensors (Thenkabail et al., 2011). Much greater details of wide array of sensors available to gather data are presented in Chapter 1 and 2 of Volume 1 of Remote Sensing Handbook.

Table 2. Characteristics of some of the key satellite sensor data currently used in cropland mapping.

Satellite sensor	Wavelength range (μm)	Spatial resolution (m)	Spectral bands (#)	Temporal (days)	Radiometric (bits)	Data points (per hectare)
A. Hyperspectral						
<i>EO-1 Hyperion</i>			196	16	16	
VNIR	0.43-0.93	30				
SWIR	0.93-2.40	30				11.1 points for 30 m pixel (0.09 hectares per pixel)
B. Advanced multispectral						
<i>Landsat TM</i>			7/8	16	8	
Multispectral						
Band 1	0.45-0.52	30				
Band 2	0.53-0.61	30				
Band 3	0.63-0.69	30				
Band 4	0.78-0.90	30				
Band 5	1.55-1.75	30				
Band 6	10.40-12.50	120/60				44.4 points for 15 m pixel
Band 7	2.09-2.35	30				11.1 points for 30 m pixel
Panchromatic	0.52-0.90	15				2.77 points for 60 m pixel
<i>EO-1 ALI</i>			10	16	16	0.69 points for 120 m pixel
Multispectral						
Band 1	0.43-0.45	30				
Band 2	0.45-0.52	30				
Band 3	0.52-0.61	30				
Band 4	0.63-0.69	30				
Band 5	0.78-0.81	30				
Band 6	0.85-0.89	30				
Band 7	1.20-1.30	30				
Band 8	1.55-1.75	30				
Band 9	2.08-2.35	30				
Panchromatic	0.48-0.69	10				

ASTER		14	16	8	
VNIR	15				
Band 1	0.52-0.60				
Band 2	0.63-0.69				
Band 3N/3B	0.76-0.86				
SWIR	30				
Band 4	1.600-1.700				
Band 5	2.145-2.185				
Band 6	2.185-2.225				
Band 7	2.235-2.285				
Band 8	2.295-2.365				
Band 9	2.360-2.430				
TIR	90				
Band 10	8.125-8.475				
Band 11	8.475-8.825				
Band 12	8.925-9.275				
Band 13	10.25-10.95				
Band 14	10.95-11.65				
MODIS					
MOD09Q1	250	2	1	12	
Band1	0.62-0.67				
Band2	0.84-0.876				
MOD09A1	500	7*/36	1	12	
Band1	0.62-0.67				
Band2	0.84-0.876				
Band3	0.459-0.479				
Band4	0.545-0.565				
Band5	1.23-1.25				
Band6	1.63-1.65				
Band7	2.11-2.16				
<hr/>					
C. Hyperspatial					
GeoEye-1					
Multispectral	1.65	5	<3	11	59,488 points for 0.41 m
Band 1	0.45-0.52				26,874 points for 0.61 m
Band 2	0.52-0.60				10,000 points for 1 m
Band 3	0.63-0.70				3673 points for 1.65 m
Band 4	0.76-0.90				1679 points for 2.44 m
Panchromatic	0.45-0.90	0.41			625 points for 4 m
IKONOS					
Multispectral	4	5	3	11	400 points for 5 m
Band 1	0.45-0.52				236 points for 6.5 m
Band 2	0.51-0.60				100 points for 10 m
Band 3	0.63-0.70				
Band 4	0.76-0.85				
Panchromatic	0.53-0.93	1	5	1-6	
Quickbird				11	

Multispectral		2.44			44.4 points for 15 m
Band 1	0.45-0.52				1.23 points for 90 m
Band 2	0.52-0.60				0.69 points for 120 m
Band 3	0.63-0.69				0.16 points for 250 m
Band 4	0.76-0.90				
Panchromatic	0.45-0.90	0.61	5	1-6	0.04 points for 500 m
<i>Rapideye</i>		5-6.5		16	
Band 1	0.44-0.51				
Band 2	0.52-0.59				
Band 3	0.63-0.68				
Band 4	0.69-0.73				
Band 5	0.76-0.85				

* MODIS 500m (Mod09A1) has 36 bands, but we considered only the first 7 bands.

5.2 Secondary data: There are wide array of secondary or ancillary data such as the ASTER derived digital elevation data (GDEM), long (50 to 100 year) records of precipitation and temperature, soil types, and administrative boundaries. Many secondary data are known to improve crop classification accuracies. The secondary data will also form core data for the spatial decision support system and final visualization tool in many systems.

5.3 Field-plot Data: Field-plot data (e.g., Figure 4) will be used for purposes such as: (i) Class identification and labeling; (ii) Determining irrigated area fractions, and (iii) Establishing accuracies, errors, and uncertainties. At each point (e.g., Figure 3) data such as cropland or non-cropland, watering method (irrigated or rainfed), crop type, and cropping intensities are gathered along with GPS locations, digital photographs, and other information (e.g., yield, soil type) as needed. Field plot data will also help us gather an ideal spectral data bank of croplands. One could use the precise locations and the crop characteristics and generate remote sensing data characteristics (e.g., MODIS time-series monthly NDVI).

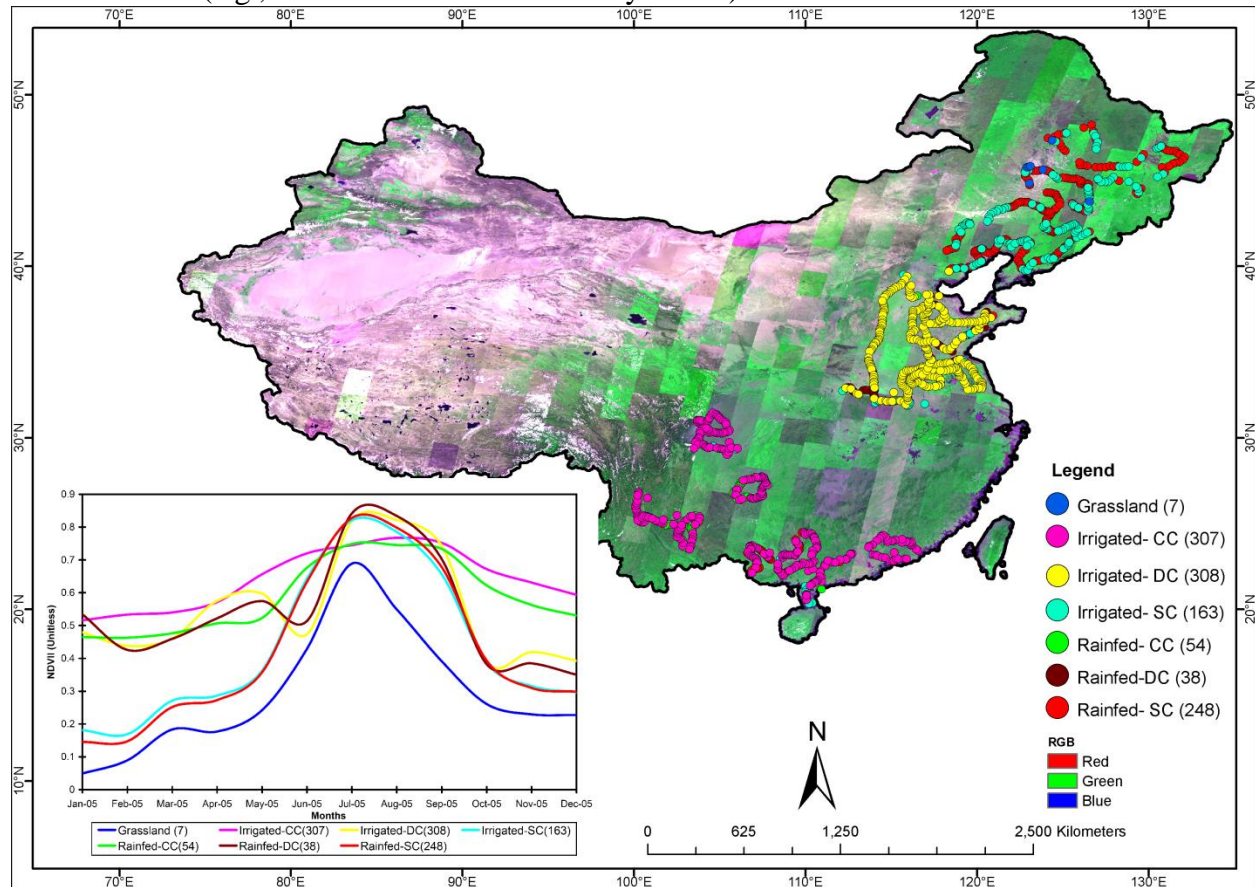


Figure 4. Field plot data for cropland studies illustrated for China.

5.4 Very high resolution imagery data

Very high resolution (sub-meter to 5 meter) imagery (VHRI; see hyperspatial data characteristics in Table 2) are widely available these days from numerous sources. These data, often act as ground sampled to classify as well as verify classification results of the coarser resolution imagery. For example, in Figure 5, VHRI tiles identify uncertainties existing in cropland classification of coarser resolution imagery. These days, VHRI are available for large parts of the world from one or the other sensors (hyperspatial, Table 2). VHRI are specifically useful for identifying croplands versus non-croplands (Figure 5). But, they can also be used for identifying irrigation (based on features such as canals, tanks).

5.5 Data composition: Mega File Data Cube (MFDC) concept

Data pre-processing would involve that all the acquired imagery is harmonized and standardized in known time intervals (e.g., monthly, bi-weekly). For this, the imagery data is either acquired or converted to at-sensor reflectance (see Chander et al., 2009, Thenkabail et al., 2004) and then converted to surface reflectance using Landsat Ecosystem Disturbance Adaptive Processing System (LEDAPS) processing system codes for Landsat or similar codes for other sensors. All data is processed to required geographic levels (e.g., global, continental). Numerous secondary datasets such as: (a) ASTER refined digital elevation from SRTM (GDEM), (b) monthly long-term precipitation, (c) monthly thermal skin temperature, (d) forest cover and density will be used for mega-file data cube (MFDC) image segmentation into distinct precipitation-elevation-temperature-vegetation zones. For example, the likelihood of croplands in a temperature zone of <280 degree Kelvin is very low. Similarly, croplands in elevation above 1500 m will be of distinctive characteristics (e.g., patchy, on hilly terrain most likely plantations of coffee or tea). Creating distinctive segments of MFDCs and analyzing them separately for croplands will enhance accuracy. Every layer of data is geo-linked (having precisely same projection and datum and are geo-referenced to one another).

The idea of mega-file data cube (MFDC; see Thenkabail et al., 2009b for details) is to ensure numerous remote sensing and secondary data layers are all stacked one over the other to form a data cube akin to hyper spectral data cube. This allows us to have the entire data stack for any geographic location (global to local) as single file available for analysis at one go. For example, one can classify 10s or 100s or even 1000s of data layers (e.g., monthly MODIS NDVI time series data for a geographic area for an entire decade along with secondary data of the same area) stacked together in a single file and classify the image. The classes coming out of such a image tell us the phenology along with providing other characteristics.

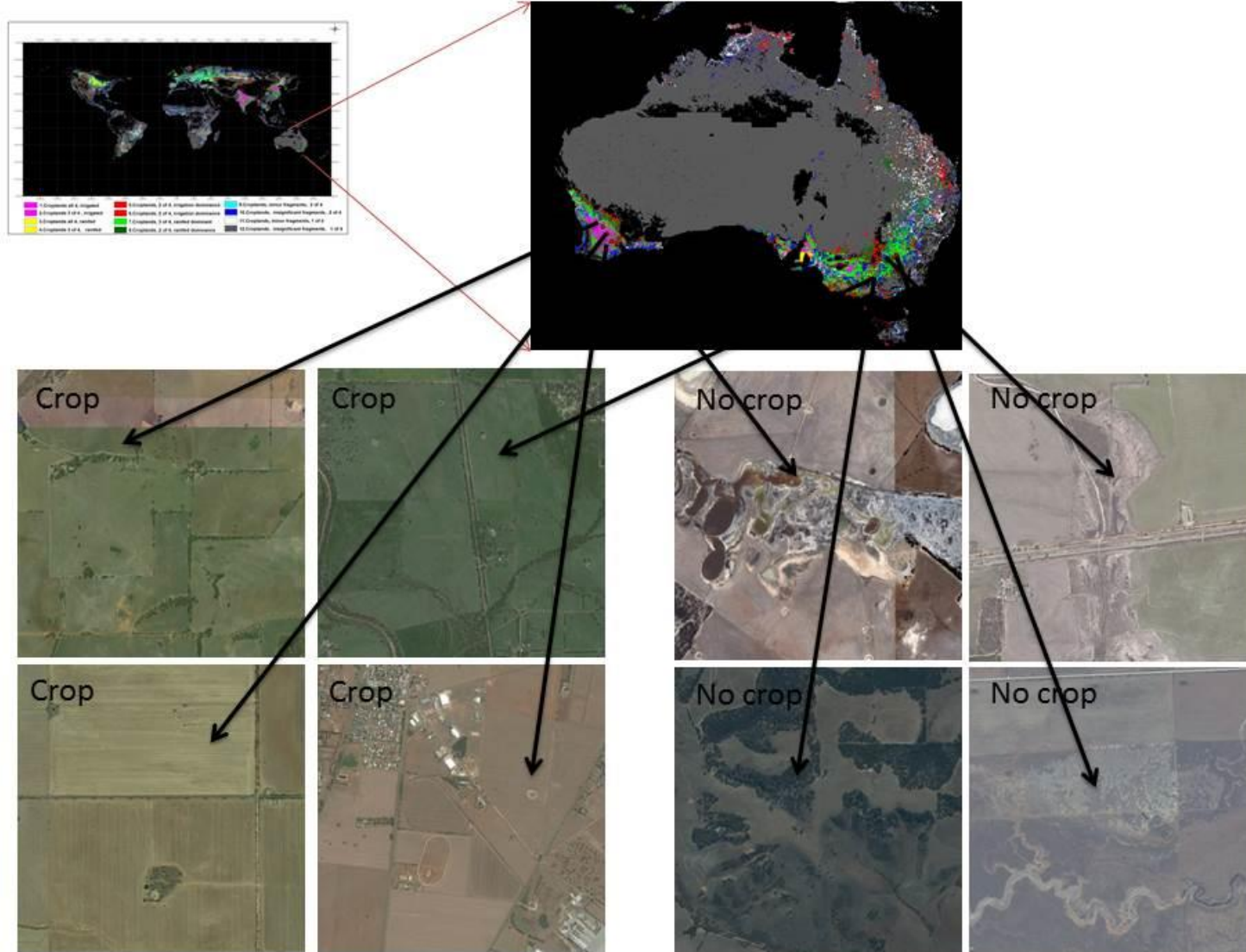


Figure 5. Very high resolution imagery showing uncertainties in cropland mapping produced using very high resolution data.

6.0 Methods of cropland mapping

6.1 Cropland mapping methods using remote sensing at global, regional, and local scales

There is growing literature on cropland (irrigated and rainfed) mapping across resolutions (Gumma et al., 2011; Friedl et al., 2002; Hansen et al., 2002; Loveland et al., 2000; Ozdogan and Woodcock, 2006; Thenkabail et al., 2009a; Thenkabail et al., 2009c; Wardlow and Egbert, 2008; Wardlow et al., 2007; Wardlow et al., 2006). Based on these experiences, an ensemble of methods that is considered most efficient includes: (a) spectral matching techniques (SMTs) (Thenkabail et al., 2007a; Thenkabail et al., 2009a; Thenkabail et al., 2009c); (b) decision tree algorithms (DeFries et al., 1998); (c) Tassel cap brightness-greenness-wetness (Cohen and Goward, 2004; Crist and Cicone, 1984; Masek et al., 2008); (d) Space-time spiral curves, Change Vector Analysis (CVA) (Thenkabail et al., 2005); (e) Phenology (Loveland et al., 2000; Wardlow et al., 2006); and (f) fusing climate data with MODIS time-series spectral indices and using algorithms such as decision tree algorithms, and sub pixel calculation of the areas (Ozdogan and Gutman, 2008). More recently, more structured cropland mapping algorithms (CMAs) are appearing. One such approach, used for global mapping by Thenkabail et al., (2009a, 2011), is described below:

6.1.1 Spectral Matching Techniques (SMTs) Algorithms (Thenkabail et al., 2007a, 2009a, b, 2011; see illustration in Figure 6, 7a);

6.1.1.1 Spectral Matching Techniques (SMTs): SMTs (Thenkabail et al., 2007a, 2009a, 2011) are innovative methods of identifying and labeling classes. For each Landsat 30-m derived class, we will look through its characteristics over time using MODIS time-series data (e.g., Figure 6). The time-series of NDVI or other metrics (Thenkabail et al., 2005, 2007a, Biggs et al., 2006, Dheeravath et al., 2010) are analogous to spectra, where time is substituted for wavelength. The principle in SMT is to match the shape, or the magnitude or both to an ideal or target spectrum (pure class or “end-member”). We will use the following quantitative SMTs (Thenkabail et al., 2007a): (a) Spectral Correlation Similarity (SCS)-a shape measure; (b) Spectral Similarity Value (SSV)-a shape and magnitude measure; (c) Euclidian Distance Similarity (EDS)-a distance measure; and (d) Modified Spectral Angle Similarity (MSAS)-a hyper angle measure.

6.1.2.2 Generating Class Spectra: The MFDC (section 2.3.5) of each of segment (Figure 6, 7a) is processed using ISOCLASS K-means classification to produce a large number of class spectra. In more localized applications, it is common to undertake field-plot data collection to identify and label class spectra. However, at the global scale this is not possible due to the enormous resources required to cover vast areas to identify and label classes. Therefore, we plan to use spectral matching techniques to match similar classes or to match class spectra with ideal or target spectra (e.g., Figure 6a) and then identify and label the classes (Thenkabail et al., 2007a).

6.1.2.3 Ideal Spectra Data Bank on Irrigated Areas (ISDB IA): the term “ideal or target” spectrum refers to time-series spectral reflectivity or NDVI generated for classes for which we have precise location specific ground knowledge. From these locations signatures are extracted using MFDC, synthesized, and aggregated to generate a few hundred signatures that will constitute an ISDB IA (e.g., Figure 6, 7a).

6.2 Automated Cropland Classification Algorithm (ACCA) (Thenkabail et al., 2012, Wu et al., 2014a, Wu et al., 2014b): The first part of the method of ACCA involves knowledge-capture to understand and map agricultural cropland dynamics by: (a) identifying croplands versus non-croplands and crop type\dominance based on spectral matching techniques, decision trees tassel cap bi-spectral plots, and very high resolution imagery; (b) determining watering method (e.g., irrigated or rainfed) based on temporal characteristics (e.g., NDVI), crop water requirement (water use by crops), secondary data (elevation, precipitation, temperature), and irrigation structure (e.g., canals and wells); (c) establishing croplands that are large scale (i.e., contiguous) versus small scale (i.e., fragmented); (d) characterizing cropping intensities (single, double, triple, and continuous cropping); (e) interpreting MODIS NDVI Temporal bi-spectral Plots to Identify and Label Classes; and (f) using in-situ data from very high resolution imagery, field-plot data, and national statistics (see Figure 7b for details). The second part of the method establishes accuracy of the knowledge-captured agricultural map and statistics by comparison with national statistics, field-plot data, and very high resolution imagery. The third part of the method makes use of the captured-knowledge to code and map cropland dynamics through an automated algorithm. The fourth part of the method compares the agricultural cropland map derived using an automated algorithm (classified data) with that derived based on knowledge capture (reference map). The fifth part of the method applies the tested algorithm on an independent data set of the same area to automatically classify and identify agricultural cropland classes. The sixth part of the method assesses accuracy and validates the classes derived from independent dataset using an automated algorithm.

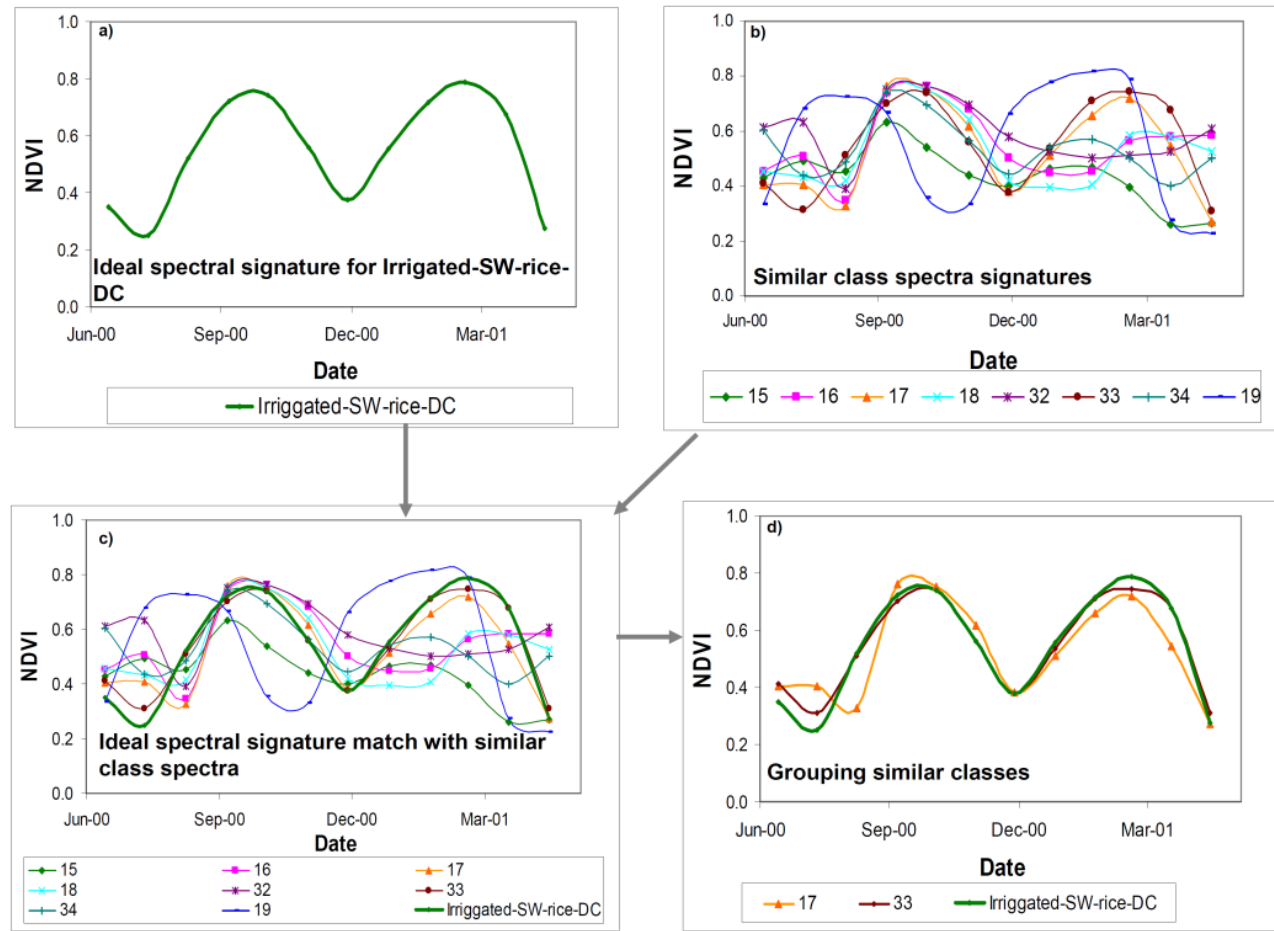


Figure 6. Spectral matching technique (SMT). In SMTs, the class temporal profile (NDVI curves) are matched with the ideal temporal profile (quantitatively based on temporal profile similarity values) in order to group and identify classes as illustrated for a rice class in this figure. a) Ideal temporal profile illustrated for “irrigated- surface-water-rice-double crop”; b) some of the class temporal profile signatures that are similar, c) ideal temporal profile signature (Fig. 6a) matched with class temporal profiles (Fig. 6b), and d) the ideal temporal profile (Fig. 6a, in deep green) matches with class temporal profiles of classes 17 and 33 perfectly. Then one can label classes 17 and 33 to be same as the ideal temporal profile (“irrigated- surface-water-rice-double crop”). This is a qualitative illustration of SMTs. For quantitative methods refer to Thenkabail et al. 2007a.

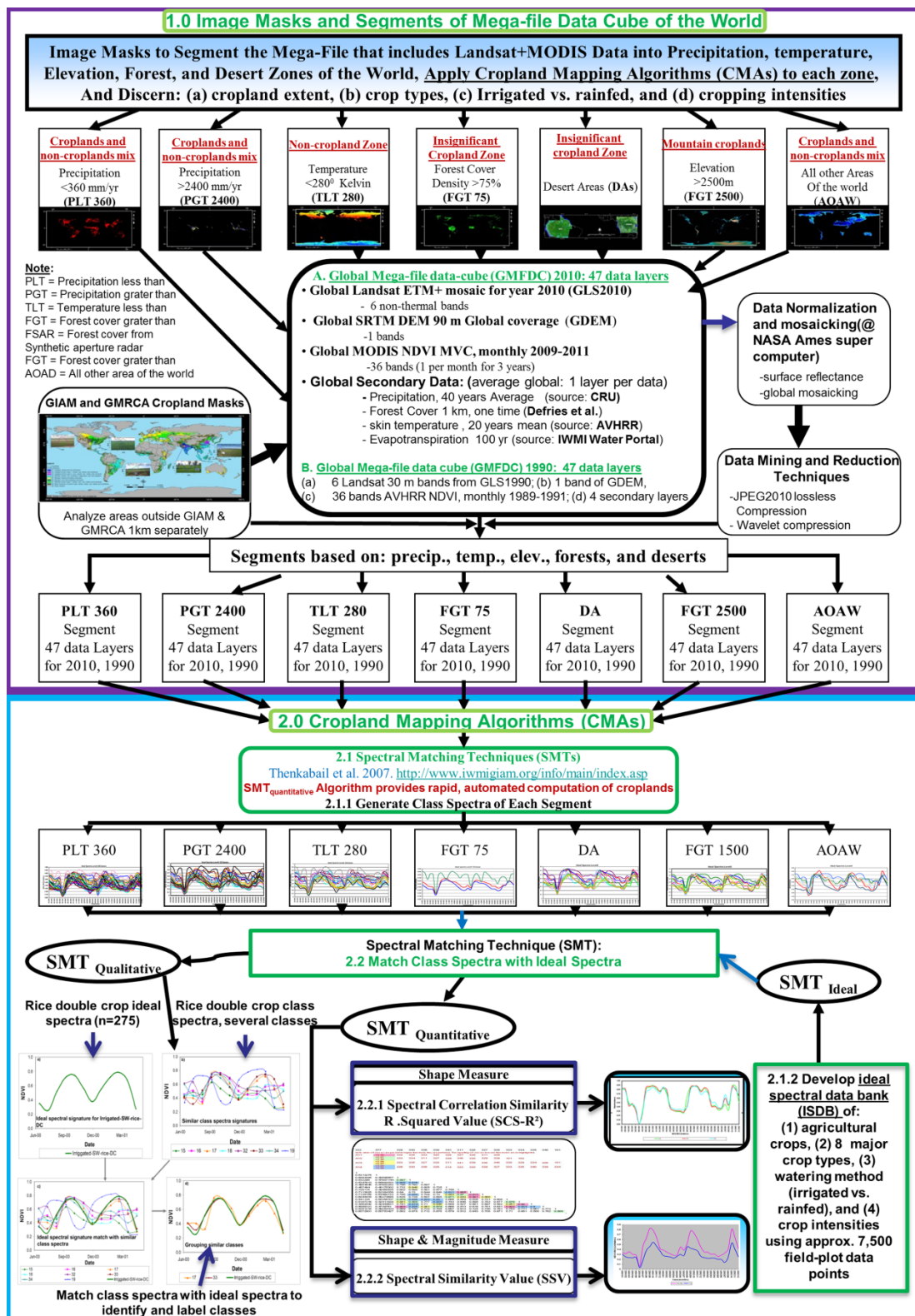


Figure 7a. Methods for mapping croplands, illustrated here for global mapping (see Thenkabail et al., 2009b, 2011). Flowchart showing comprehensive global cropland mapping methods using multi-sensor, multi date remote sensing, secondary, field plot, and very high resolution imagery data.

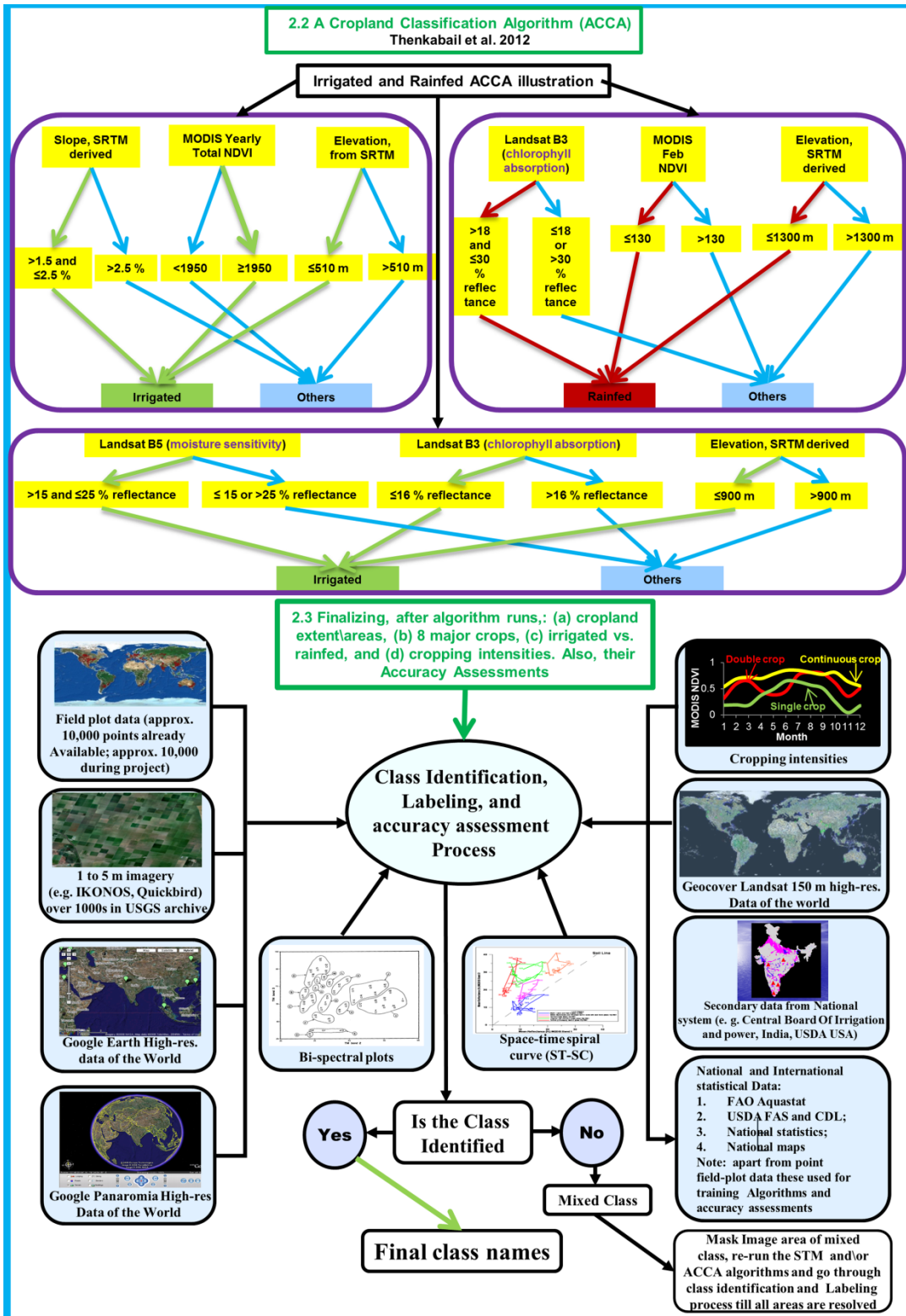


Figure 7b. Methods for mapping croplands, illustrated for global mapping. Top half shows automated cropland classification algorithm (see Thenkabail and Wu, 2012; Wu et al., 2014a) and bottom half shows class identification and labeling process.

7.0 Remote sensing based global cropland products: current state-of-art, their strengths, and limitations

Remote sensing offers the best opportunity to map and characterize global croplands most accurately, consistently, and repeatedly. Currently, there are 3 global cropland maps of the world. These maps were produced by:

- A. Thenkabail et al. (Thenkabail et al., 2009b, Biradar et al., 2009, Thenkabail et al., 2011);
- B. Pittman et al. (2010); and
- C. Yu et al., (2013);

In addition, we also considered a recent MODIS global land cover and land use map where croplands have also been mapped.

- D. Friedl et al (2010)

Thenkabail et al. (2009b, 2011; Figure 8, Table 3) used combination of AVHRR, SPOT VGT, and numerous secondary (e.g., precipitation, temperature, and elevation) data to produce global irrigated area map (Thenkabail et al., 2009b, 2011), global map of rainfed cropland areas (Biradar et al., 2009, Thenkabail et al., 2011; Figure 8, Table 3). Pittman et al. (2010; Figure 9, Table 4), used MODIS 250 m data to develop cropland extent of the world. More recently, Yu et al. (2013; Figure 10, Table 5), produced a nominal 30 m resolution cropland extent of the world. These three global cropland extent maps are the best available current state-of-art. In addition we also used croplands mapped at 500 m using MODIS data by Friedl et al. (2010; Figure 11, Table 6) in their global land cover and land use product (MCD12Q1). The methods, approaches, data, and definitions used in each of these products differ extensively. As a result, the cropland extents mapped by these products also vary significantly. The areas in the Tables only show the full pixel areas (FPAs) and not sub-pixel areas (SPAs). SPAs will be actual areas. Further, actual areas are determined by re-projecting these maps to appropriate projections and calculating the areas. It was thought this is not necessary at this stage. However, just a comparison of the FPAs (Table 3 to 6) of the 4 maps (Figure 8 to 11) show significant differences in the cropland areas (Table 3 to 6) as well as significant differences in the precise locations of the croplands (Figure 8 to 11). The reasons for which are discussed in next section.

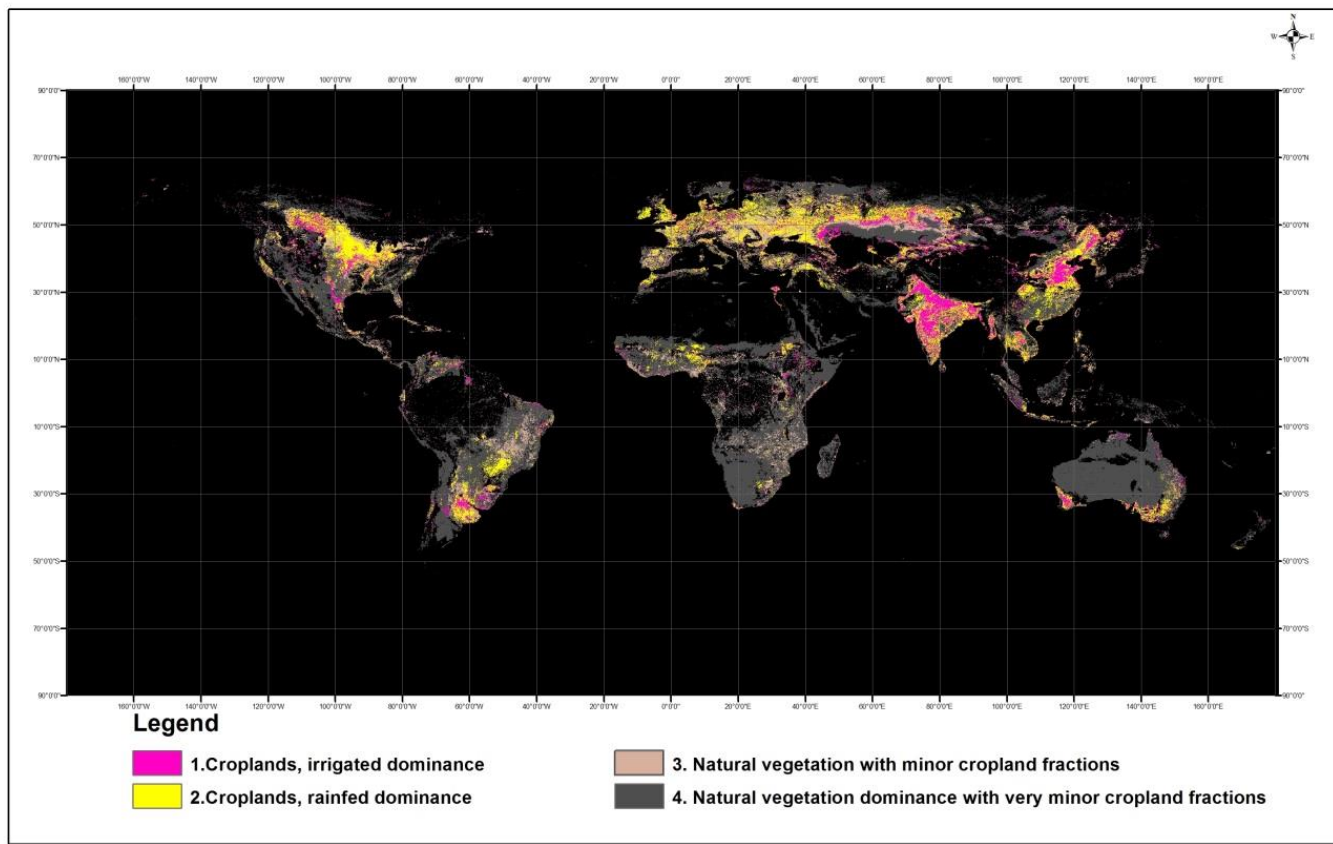


Figure 8. Global cropland product by Thenkabail et al., (2011, 2009b) using method illustrated in Figure 6a and 6b and described in section 3.2.1 (details in Thenkabail et al., 2011, 2009b). This includes irrigated and rainfed areas of the world as well as permanent crops. The product is derived using remotely sensed data fusion (e.g., NOAA AVHRR, SPOT VGT, JERS SAR), secondary data (e.g., elevation, temperature, and precipitation), and in-situ data. Total area of croplands is 2.3 billion hectares.

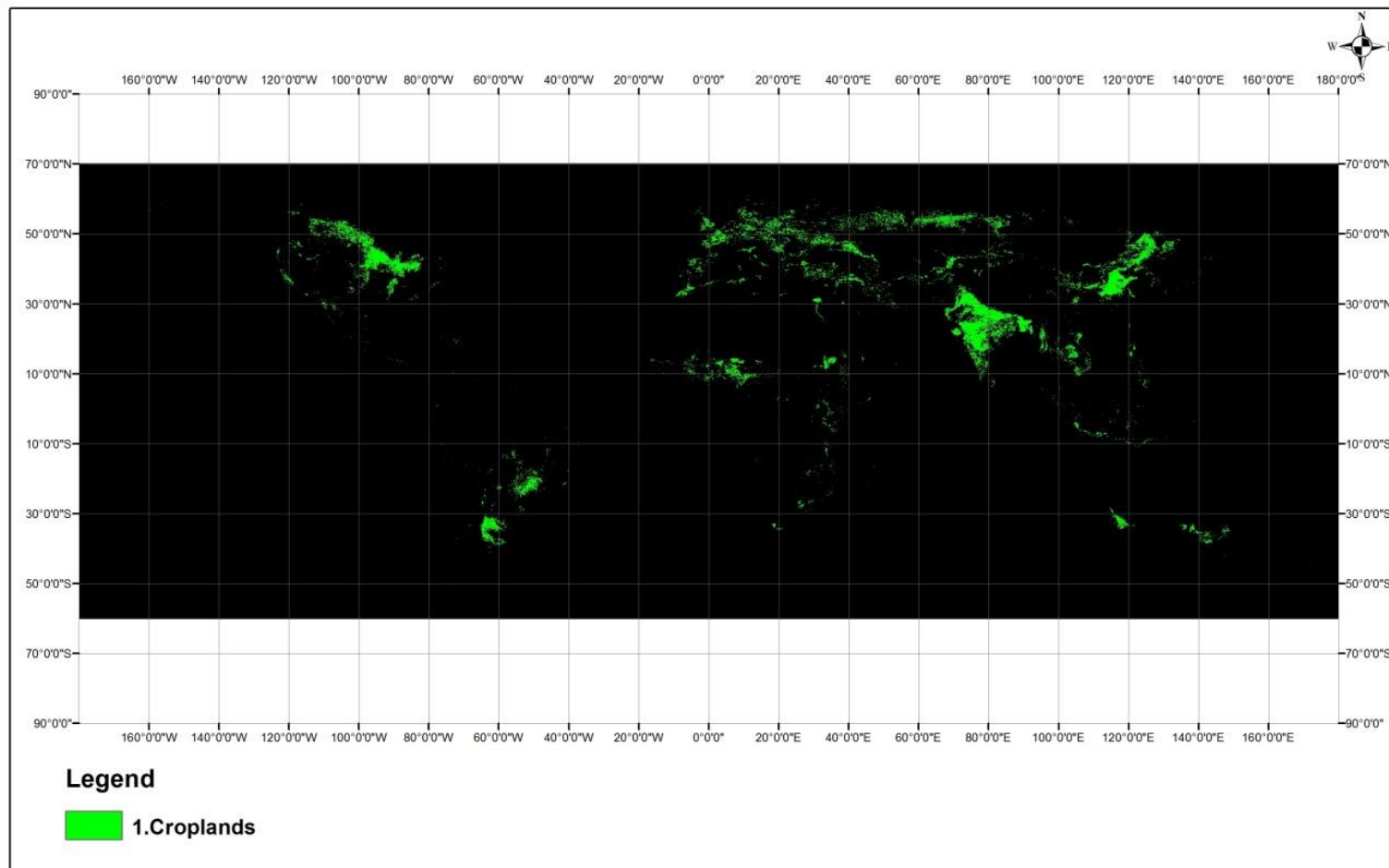


Figure 9. Global cropland extent product by Pittman et al. (2010) derived using MODIS 250 m data. There is only one cropland class, this includes irrigated and rainfed areas of the world, there is no discrimination between rainfed and irrigated areas. Total area of croplands is 0.9 billion hectares.

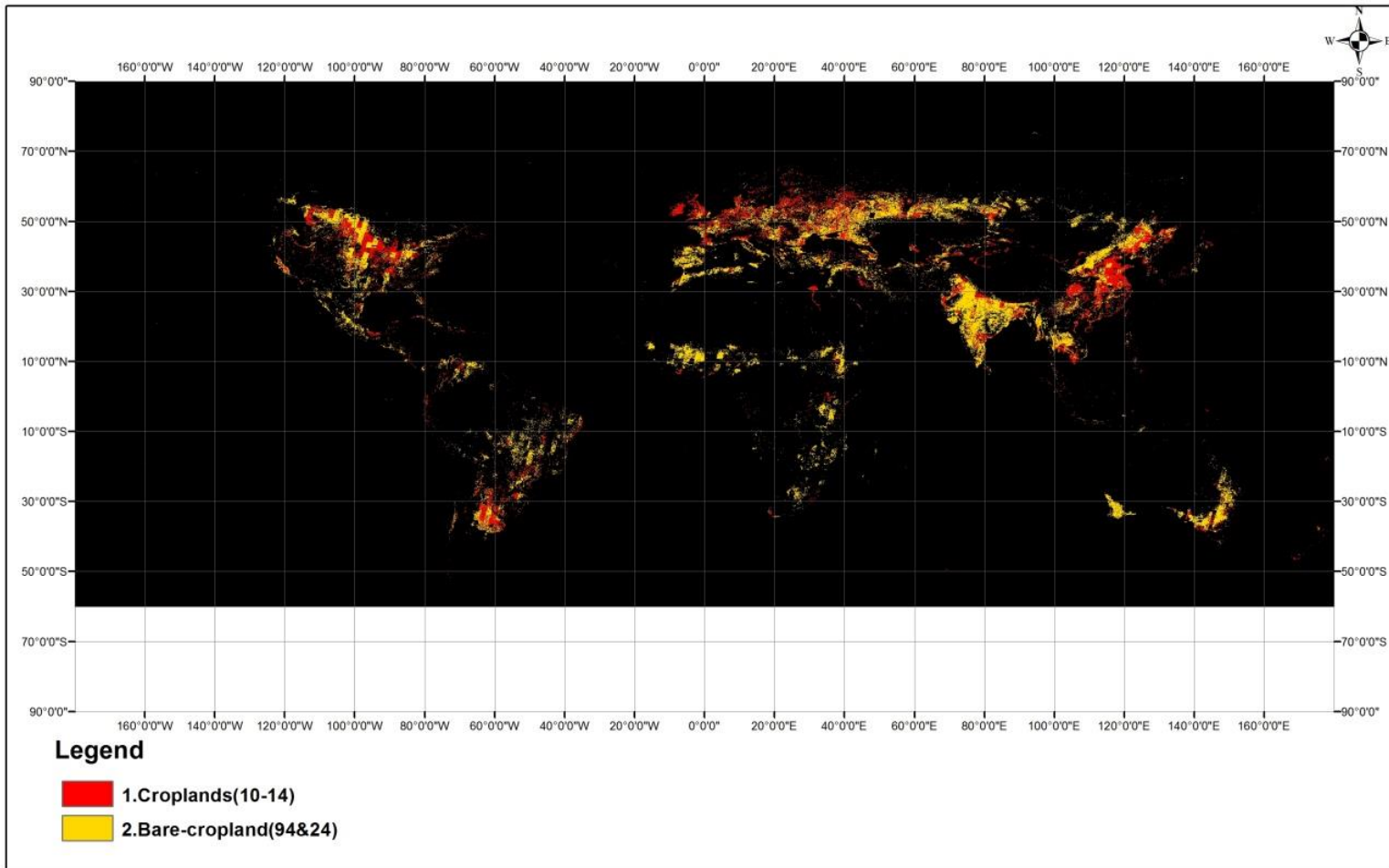


Figure 10. Global cropland extent product by Yu et al. (2013) derived at nominal 30m data. Total area of croplands is 2.2 billion hectares. there is no discrimination between rainfed and irrigated areas.

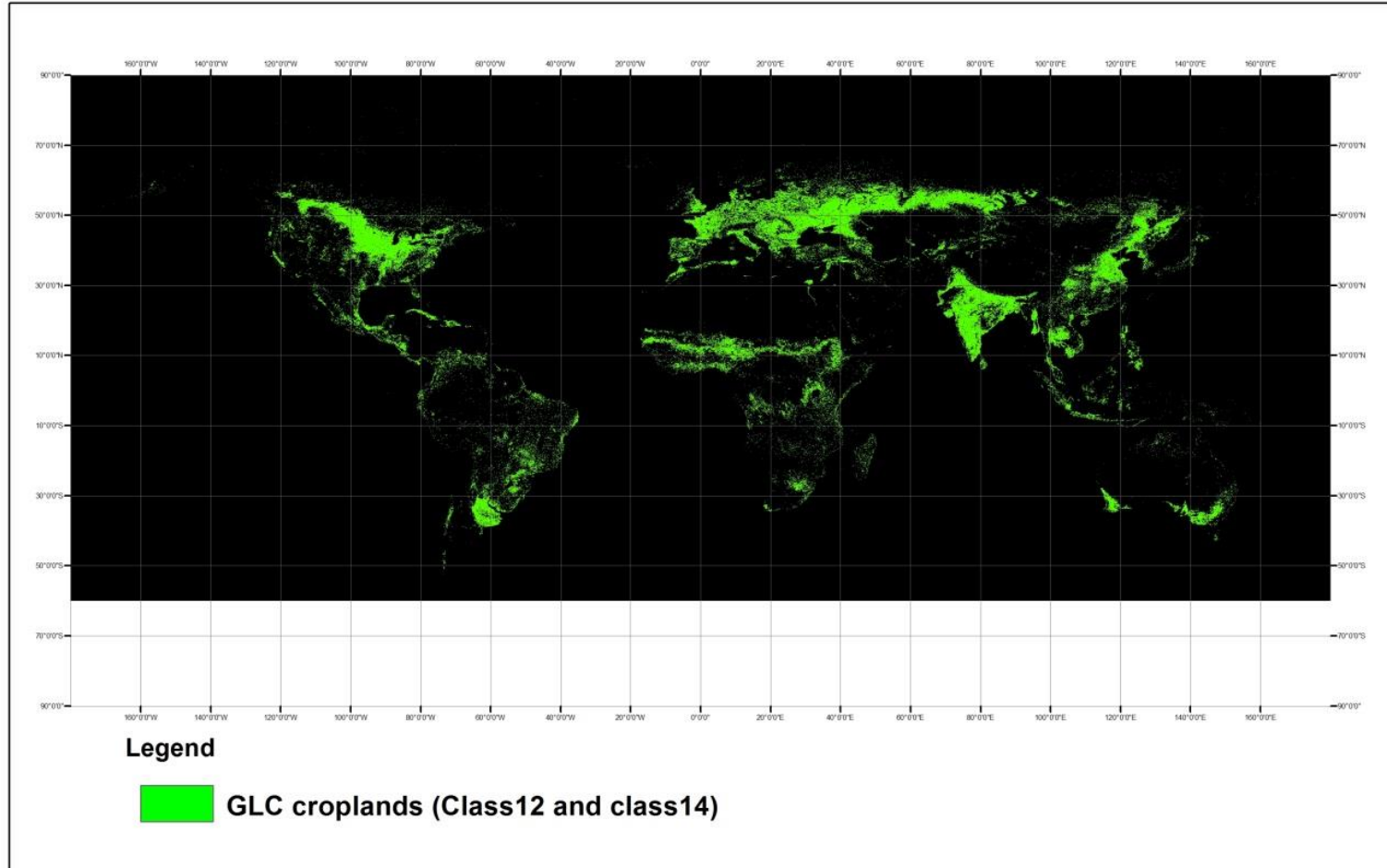


Figure 11. Global cropland classes (Class12 and Class14) extracted from MODIS Global land use and land cover (GLC) 500m product MCD12Q2 by Friedl et al. (2010). Total area of croplands is 2.7 billion hectares. There is no discrimination between rainfed and irrigated cropland areas.

Table 3. Global cropland extent at nominal 1-km based on Thenkabail et al. (2009b, 2011)^{1,2}.

Class#	Class Description	Pixels	Percent
#	Names	unitless	%
1	Croplands, irrigated dominance	9359647	40%
2	Croplands, rainfed dominance	14273248	60%
3	Natural vegetation with minor cropland fractions	5504037	
4	Natural vegetation dominance with very minor cropland fractions	44170083	
		23632895	100%
Note:			
1 = approximately, total 2.3 billion hectares; Note that these are full pixel areas (FPAs). Actual area is = sub-pixel area (SPA). The SPA is not estimated here. See Thenkabail et al. (2007b) for the methods for calculating SPAs.			
2 = % calculated based on class 1 and 2. Class 3 and 4 are very small cropland fragments			

Table 4. Global cropland extent at nominal 250 m based on Pittman et al. (2010)^{1,2}.

Class#	Class Description	Pixels	Percent
#	Names	unitless	%
1	Croplands	8948507	100
Note:			
1 = approximately, total 0.9 billion hectares. Note that these are full pixel areas (FPAs). Actual area is = sub-pixel area (SPA). The SPA is not estimated here. See Thenkabail et al. (2007b) for the methods for calculating SPAs.			
2 = % calculated based on class 1			

Table 5. Global cropland extent at nominal 30 m based on Yu et al. (2013)^{1,2}.

Class#	Class Description	Pixels	Percent
#	Names	unitless	%
1	Croplands (classes 10 to 14)	7750467	35
2	Bare-cropland(classes 94 and 24)	14531323	65
		22281790	100
Note:			
1 = approximately, total 2.2 billion hectares. Note that these are full pixel areas (FPAs). Actual area is = sub-pixel area (SPA). The SPA is not estimated here. See Thenkabail et al. (2007b) for the methods for calculating SPAs.			
2 = % calculated based on class 1 and 2.			

Table 6. Global cropland extent at nominal 500 m based on Friedl et al. (2010)¹.

Class#	Class Description	Pixels	Percent
#	Names	unitless	%
1	Global croplands (Class 12 and 14)	27046084	100
Note:			
Note:			
1= approximately, total 2.7 billion hectares based on class12 and 14. Note that these are full pixel areas (FPAs). Actual area is = sub-pixel area (SPA). The SPA is not estimated here. See Thenkabail et al. (2007b) for the methods for calculating SPAs.			

7.1 Global cropland extent at nominal 1-km resolution

We synthesized the above 4 global cropland products and produced a unified global cropland extent map at nominal 1 km and called it GCE V1.0 (Table 7a; Figure 12a). The process involved, resampling each global cropland product to a common resolution of 1 km and then performing GIS data overlays to determine where the cropland extent mapped by these products match and where they differ.

The Figure 12a shows the aggregated global cropland extent map with its statistics in Table 7a. Class 1 in Figure 12a and Table 7a provides the global cropland extent mapped by all 4 maps. Actual area of this extent is not calculated as yet, but roughly there is about 2.3 billion full pixel areas (FPAs) (Table 7a). The spatial distribution of these 2.3 billion hectares is shown by class 1 of Figure 12a. Class 2 and 3 are areas with minor or insignificant cropland fractions. Class 2 and Class 3 are classes with large areas of natural vegetation and/or desert lands and other lands.

Figure 12b and Table 7b tell us where and by how much each of the 4 products matches. For example, 2,802,397 pixels (class 1, Table 7b, Figure 12b) are croplands that are irrigated. Actually, some of the products do not identify irrigated from rainfed. But, all 4 products show where croplands are. So, we too have that information to see where all 4 products match as croplands and then added irrigated or other indicators (e.g., irrigation dominance, rainfed; Table 7b) from the work of Thenkabail et al.

Table 7b and Figure 12b show 12 classes of which class 1 and 2 are croplands with irrigated agriculture, class 3 and 4 are croplands with rainfed agriculture, class 5 and 6 are croplands where irrigated agriculture dominates, class 7 and 8 are croplands where rainfed agriculture dominates, and class 9 to 12 are areas with minor or insignificant cropland fractions. Classes 9 to 12 are classes with large areas of natural vegetation and/or desert lands and other lands.

What is interesting, and surprising as well, is that only 20% (class 1 and 3; Table 7b, Figure 12b) of the total cropland extent are matched precisely in all 4 products. Further, 49% (Class 1, 2, 3, 4, and 7; Table 7b, Figure 12b) of the total cropland areas match in atleast 3 of the 4 products. What this implies is that all the 4 products have considerable uncertainties in determining the precise location of the croplands. The great degree of uncertainty in the cropland products can be attributed to factors such as:

- A. Coarse resolution of the imagery used in the study;
- B. Definition of mapping;
- C. Methods used;
- D. Approaches adopted;
- E. Limitations of the data such as saturation;

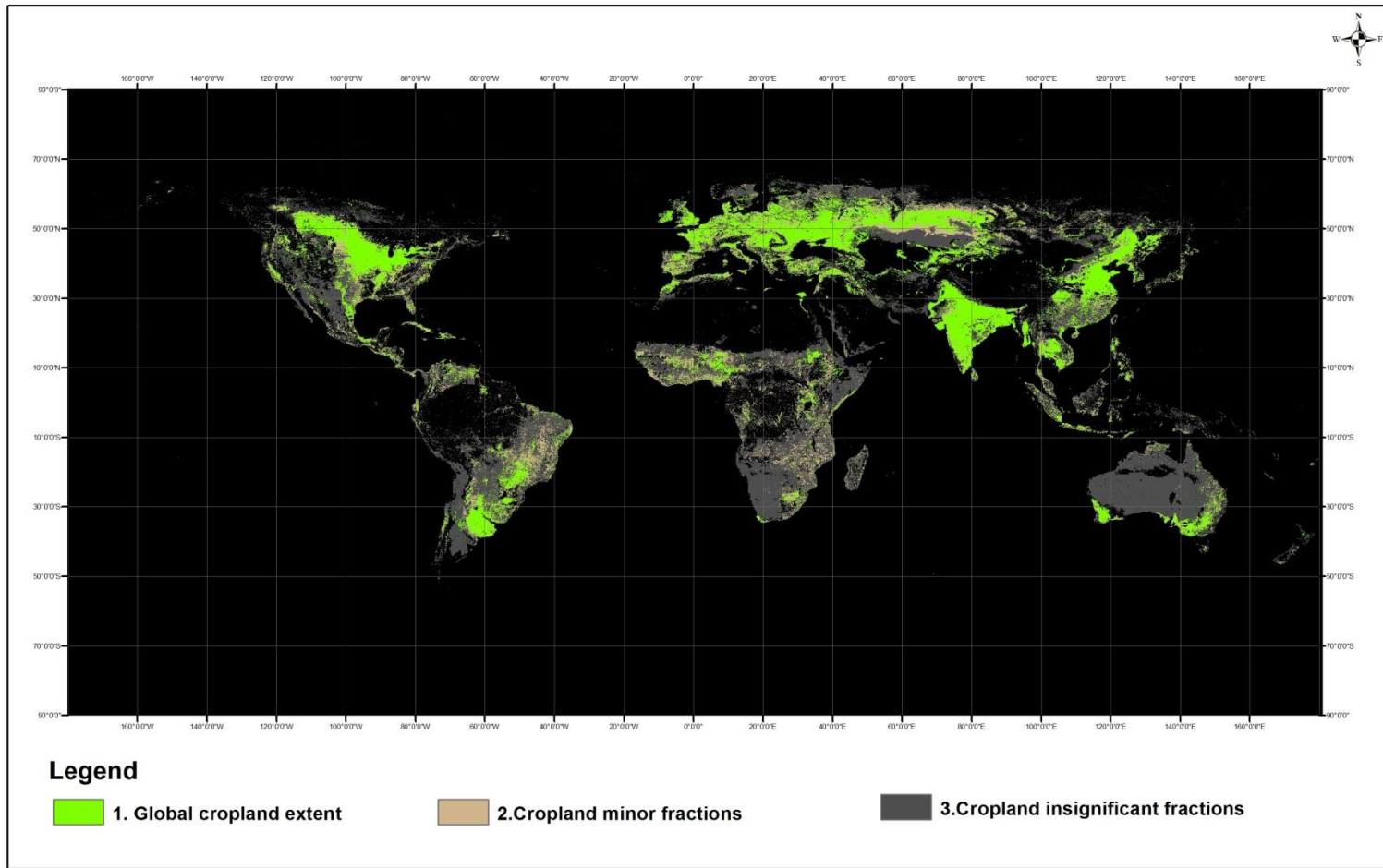


Figure 12a. An aggregated three class global cropland extent map at nominal 1-km based on four major studies: Thenkabail et al. (2009a, 2011), Pittman et al. (2010), Yu et al. (2013) and Friedl et al. (2010). Class 1 is total cropland extent; total cropland extent is 2.3 billion hectares (full pixel areas). Class2 and Class3 have minor fractions of croplands.

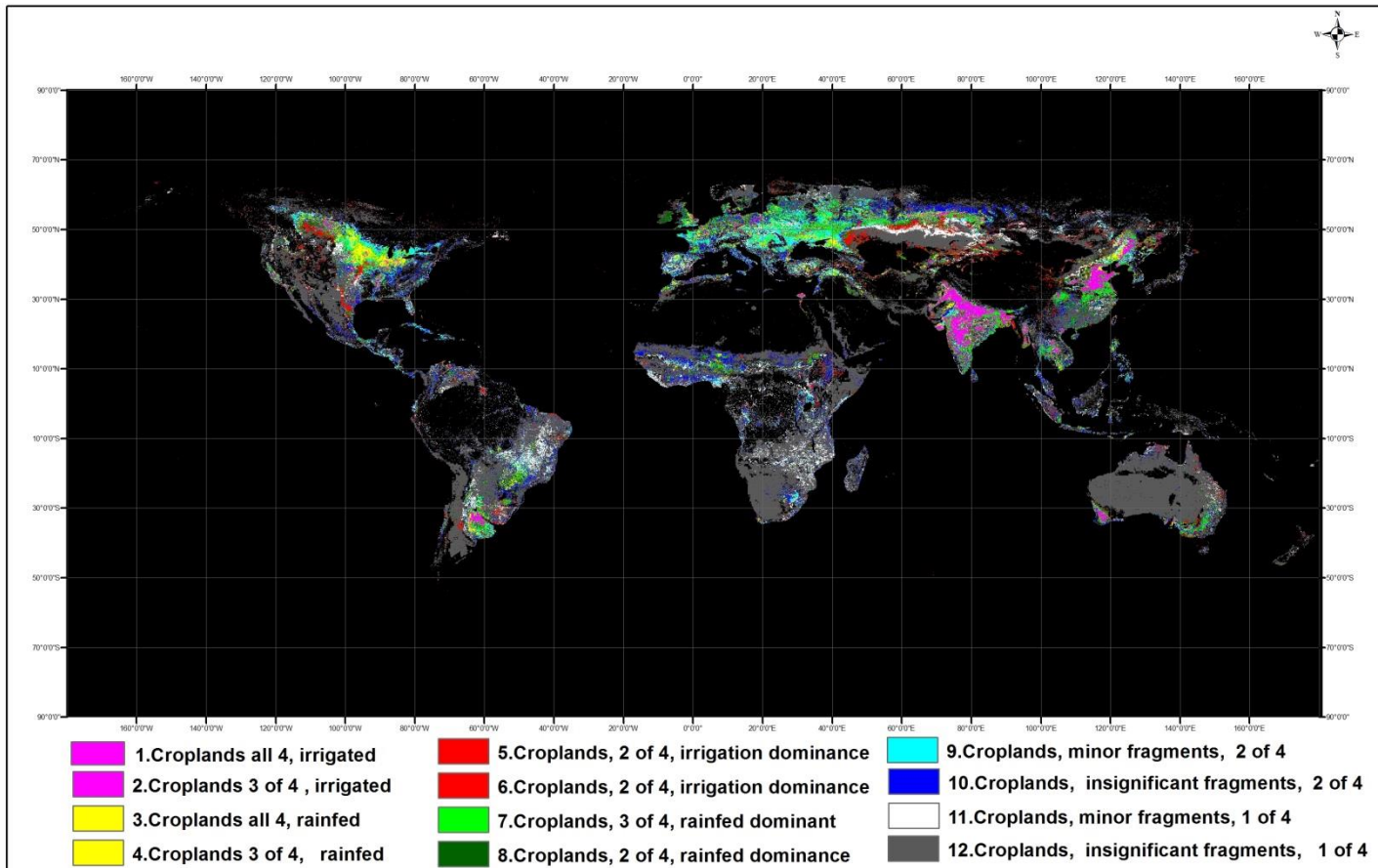


Figure 12b. A disaggregated twelve class global cropland extent map derived at nominal 1-km based on four major studies: Thenkabail et al. (2009a, 2011), Pittman et al. (2010), Yu et al. (2013) and Friedl et al. (2010). Class1 to Class 9 are cropland classes, basically these classes shows dominance of irrigated and rainfed agriculture. Class10 to and Class 12 have minor/very minor fractions of croplands.

Table 7a. Global cropland extent at nominal 1-km based on four major studies: Thenkabail et al. (2009b, 2011), Pittman et al. (2010), Yu et al. (2013), and Friedl et al.(2010). Three class map^{1,2,3}.

Class#	Class Description	Pixels	Percent
#	Names	unit less	%
1	1. Global cropland extent	23493936	100
2	2.Cropland minor fractions	13700176	
3	3.Cropland insignificant fractions	44662570	
Note:			
1=	approximately 2.3 billion hectares (class 1) of cropland is estimated. But this is full pixel area. Actual area is = sub-pixel area (SPA). The SPA is not estimated here. See Thenkabail et al. (2007b) for the methods for calculating SPAs.		
2=	% calculated based on Class 1.		
3=	Class 2 and 3are minor /insignificant cropland fragments		

Table 7b. Global cropland extent at nominal 1-km based on four major studies: Thenkabail et al. (2009b, 2011), Pittman et al. (2010), Yu et al. (2013), and Friedl et al. (2010). Twelve class map^{1,2,3,4}.

Class#	Class Description	Pixels	Percent
#	Names	unit less	%
1	Croplands all 4, irrigated	2802397	12
2	Croplands 3 of 4 , irrigated	289591	1
3	Croplands all 4, rainfed	1942333	8
4	Croplands 3 of 4, rainfed	427731	2
5	Croplands, 2 of 4, irrigation dominance	3220330	14
6	Croplands, 2 of 4, irrigation dominance	1590539	7
7	Croplands, 3 of 4, rainfed dominant	6206419	26
8	Croplands, 2 of 4, rainfed dominance	3156561	13
9	Croplands, minor fragments, 2 of 4	3858035	17
10	Croplands, insignificant fragments, 2 of 4	6825290	
11	Croplands, minor fragments, 1 of 4	6874886	
12	Croplands, insignificant fragments, 1 of 4	44662570	
	Class 1 to 9 total	23493936	100
Note:			
1=	approximately 2.3 billion hectares (class 1 to 9) of cropland is estimated. But this is full pixel area. Actual area is = sub-pixel area (SPA). The SPA is not estimated here. See Thenkabail et al. (2007b) for the methods for calculating SPAs.		
2=	% calculated based on class 1 to 9		
3=	Class 10,11and 12 are minor cropland fragments		
4=	all 4 means , all 4 studies agreed		

8.0 Change Analysis: Once the crop lands are mapped (Figure 13), we will use the time-series historical data such as continuous global coverage of remote sensing data from NOAA Very High Resolution Radiometer (VHRR) and Advanced VHRR (AVHRR) Global Inventory Modeling and Mapping Studies (GIMMS; 1982-2000), MODIS time-series (2001-present) to help build an inventory of history agricultural development (e.g., Figure 13, 14) by providing information on such factors as which areas have switched from rainfed to irrigated production (full or supplemental), non-cropped to cropped (and vice versa). A complete history will require systematic analysis of remotely sensed data as well as a systematic compilation of all routinely populated cropland databases from the agricultural departments of all countries throughout the world. The differences in pixel sizes in AVHRR *versus* MODIS will: (a) influence class identification and labeling, and (b) cause different levels of uncertainties. We will address these issues by determining sub-pixel areas and uncertainties involved in class accuracies and uncertainties in areas at various spatial resolutions explained in detail recent work of this team (Thenkabail et al. 2007b, Velpuri et al., 2009, and Ozdogan and Woodcock 2006). Change analysis (Tomlinson, 2003) are conducted in order to investigate both the spatial and temporal changes in croplands (e.g., Figure 13, 14) that will help establish: (a) change in total cropland areas, (b) change in spatial location of cropland areas, (c) expansion on croplands into natural vegetation, (d) expansion of irrigation, (e) change from croplands to bio-fuels, and (f) change from croplands to urban. Massive reductions in cropland areas in certain parts of the world, for example, reductions in available ground water supply as a result of overdraft (Wada et al., 2012, Rodell et al., 2010) will be established for the quantum of areas lost, and regions where such areas are lost.

9.0 Limitations of existing cropland products: Currently, the main causes of uncertainties in areas reported in various studies can be attributed to (Ramankutty et al., 2008 versus; Thenkabail et al., 2009a; Thenkabail et al., 2009c), but not limited to: (a) reluctance of national and state agencies to furnish the census data on irrigated area in view of their institutional interests in sharing of water and water data; (b) reporting of large volumes of census data with inadequate statistical analysis; (c) subjectivity involved in the observation-based data collection process; (d) inadequate accounting of irrigated areas, especially minor irrigation from groundwater, in national statistics; (e) definitional issues involved in mapping using remote sensing as well as national statistics; (f) difficulties in arriving at precise estimates of area fractions (AFs) using remote sensing; (g) difficulties in separating irrigated from rainfed croplands; and (h) imagery resolution in remote sensing. Other limitations include (Thenkabail et al., 2009a, 2011):

- A. Absence of precise spatial location of the cropland areas;
- B. Uncertainties in differentiating irrigated areas from rainfed areas;
- C. Absence of crop types and cropping intensities;
- D. Inability to generate cropland maps and statistics, routinely; and
- E. Absence of dedicated web\data portal for dissemination cropland products.

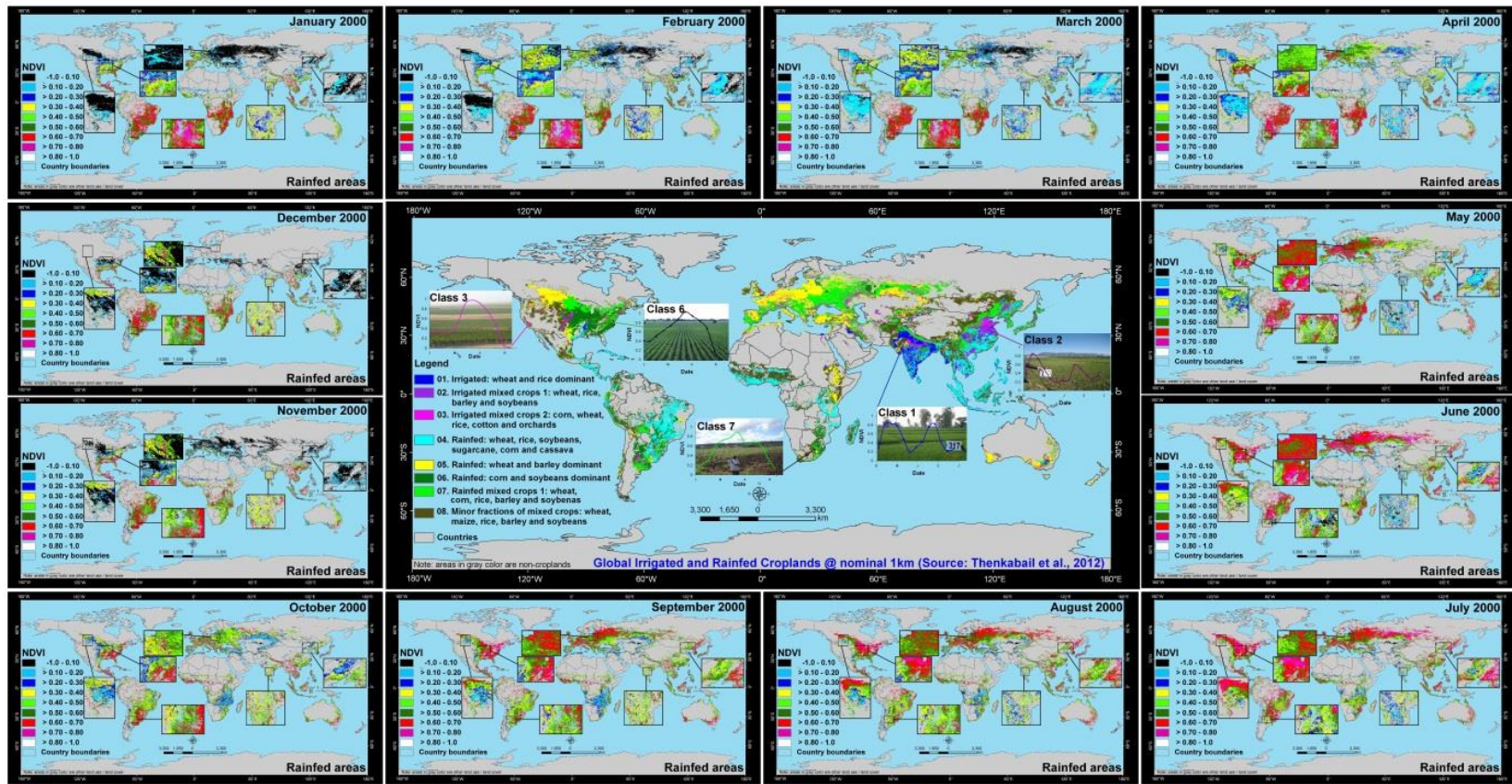


Figure 13. Center image of global cropland (irrigated and rainfed) areas @ 1 km for year 2000 produced by overlaying the remote sensing derived product of the International Water Management Institute (IWMI; Thenkabail et al., 2012, 2011, 2009a, 2009b; <http://www.iwmigiam.org>) over 5 dominant crops (wheat, rice, maize, barley and soybeans) of the world produced by Ramankutty et al. (2008). The 5 crops constitute about 60% of all global cropland areas. The IWMI remote sensing product is derived using remotely sensed data fusion (e.g., NOAA AVHRR, SPOT VGT, JERS SAR), secondary data (e.g., elevation, temperature, and precipitation), and *in-situ* data. Total area of croplands is 1.53 billion hectares of which 399 million hectares is total area available for irrigation (without considering cropping intensity) and 467 million hectares is annualized irrigated areas (considering cropping intensity). **Surrounding NDVI images of irrigated areas:** The January to December irrigated area NDVI dynamics is produced using NOAA AVHRR NDVI. The irrigated areas were determined by Thenkabail et al. (2011, 2009a, b).

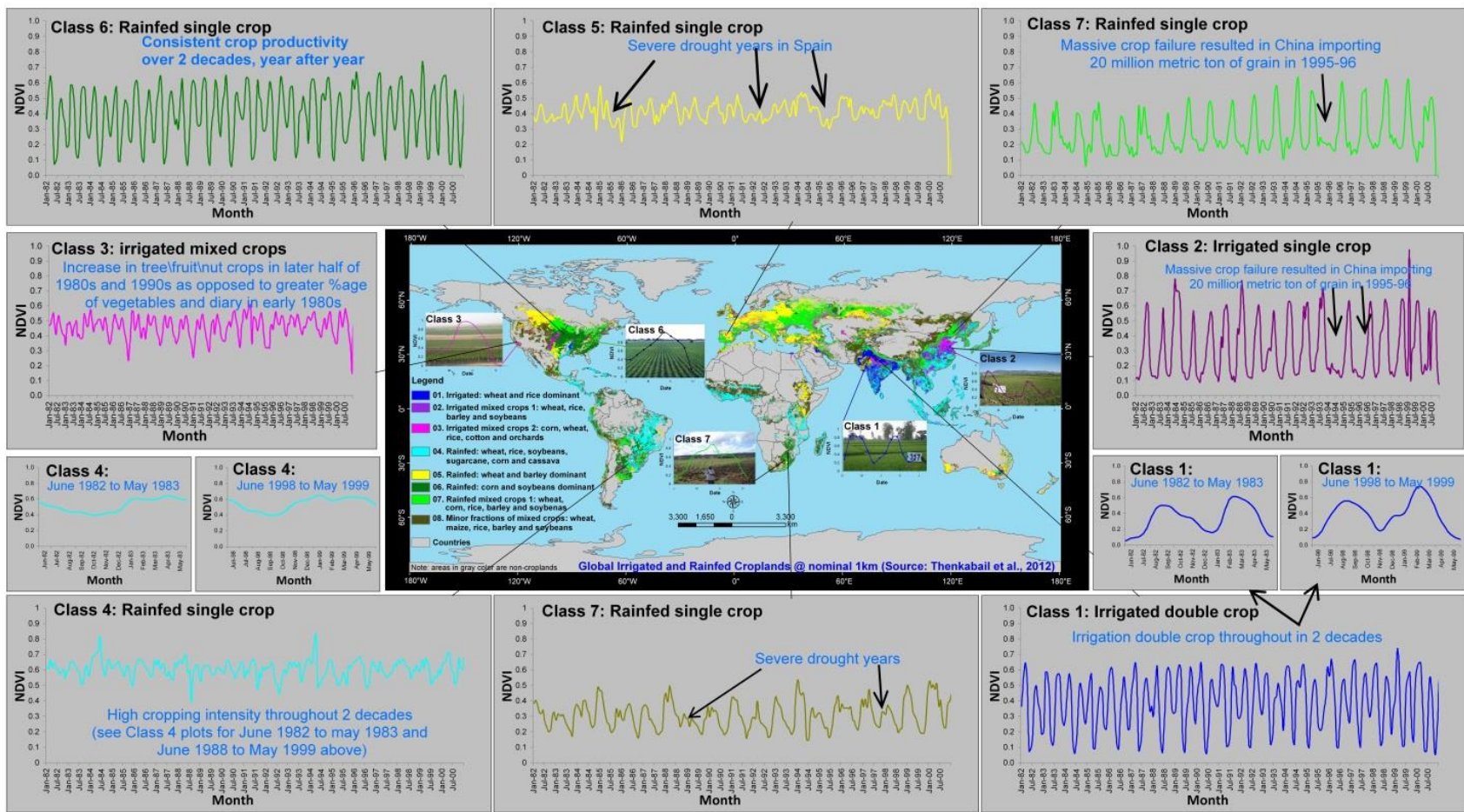


Figure 14. Global agricultural dynamics over 2 decades illustrated here for some of the most significant agricultural areas of the World. Once we establish GCAD2010 and GCAD1990 at nominal 30 m resolution for the entire world, we will use AVHRR-MODIS monthly MVC NDVI time-series from 1982 to 2017 to provide a continuous time history of global irrigated and rainfed croplands, establish their spatial and temporal changes, and highlight the hot spots of change. The **GCAD2010**, **GCAD1990**, and **GCAD four decade's** data will be made available on USGS global cropland data portal (currently under construction):
http://powellcenter.usgs.gov/current_projects.php#GlobalCroplandsAbstract.

Further, the need to map accurately, specific cropland characteristics like crop types and watering methods (e.g., irrigated vs. rainfed) is crucial in food security analysis. For example, the importance of irrigation to global food security is highlighted in a recent study by Siebert and Doll (2009) who show that without irrigation there would be a decrease in production of various foods including dates (60%), rice (39%), cotton (38%), citrus (32%) and sugarcane (31%) from their current levels. Globally, without irrigation cereal production would decrease by a massive 43%, with overall cereal production, from irrigated and rainfed croplands, decreasing by 20%.

These limitations are a major hindrance in accurate/reliable global, regional, and country by country water use assessments that in turn support crop productivity (productivity per unit of land; kg/m^2) studies, water productivity (productivity per unit of water; kg/m^3) studies, and food security analyses. The higher degrees of uncertainty in coarser resolution data are a result of an inability to capture fragmented, smaller patches of croplands accurately, and the homogenization of both crop and non-crop land within areas of patchy land cover distribution. In either case, there is a strong need for finer spatial resolution to resolve the confusion.

10.0 Way forward

Given the above issues with existing maps of global croplands, the way forward will be to produce global cropland maps at finer spatial resolution. Research has shown that at finer spatial resolution the accuracy of irrigated and rainfed area class delineations improves because at finer spatial resolution more fragmented and smaller patches of irrigated and rainfed croplands can be delineated (Ozdogan and Woodcock, 2006; Velpuri et al., 2009). Further, greater details of crop characteristics such as the crop types (e.g., Figure 15) can be determined at finer spatial resolutions. Crop type mapping will involve use of advanced methods of analysis such as, for example, fused higher spatial resolution from sensors such as Resourcesat\Landsat and AWIFS\MODIS imagery (e.g., Table 2) supported by extensive ground surveys and ideal spectral data bank (ISDB) (Thenkabail et al., 2007a). Harmonic analysis is often adopted to identify crop types (Sakamoto et al., 2005) using methods such as the conventional Fourier analysis and adopting a Fourier Filtered Cycle Similarity (FFCS) method. Mixed classes are resolved using hierarchical crop mapping protocol based on decision tree algorithm (Wardlow and Egbert, 2008). Irrigated versus rainfed croplands will be distinguished using spectral libraries (Thenkabail et al., 2007) and ideal spectral data banks (Thenkabail et al., 2009a, 2007a). Similar classes will be grouped by matching class spectra with ideal spectra based on spectral matching techniques (SMTs; Thenkabail et al., 2007a). Details such as crop types are crucial for determining crop water use, crop productivity, and water productivity leading to providing crucial information needed for food security studies. However, the high spatial resolution must be fused with high temporal resolution data in order to obtain time-series spectra that are crucial for monitoring crop growth dynamics and cropping intensity (e.g., single crop, double crop, and continuous year round crop). Numerous other methods and approaches exist. But, the ultimate goal using multi-sensor remote sensing is to produce croplands products such as:

1. Cropland extent\area,
2. Crop types (focus on 8 crops that occupy 70% of global croplands),
3. Irrigated vs. rainfed croplands,
4. Cropping intensities\phenology (single, double, triple, continuous cropping),
5. Cropped area computation; and
6. Cropland change over space and time

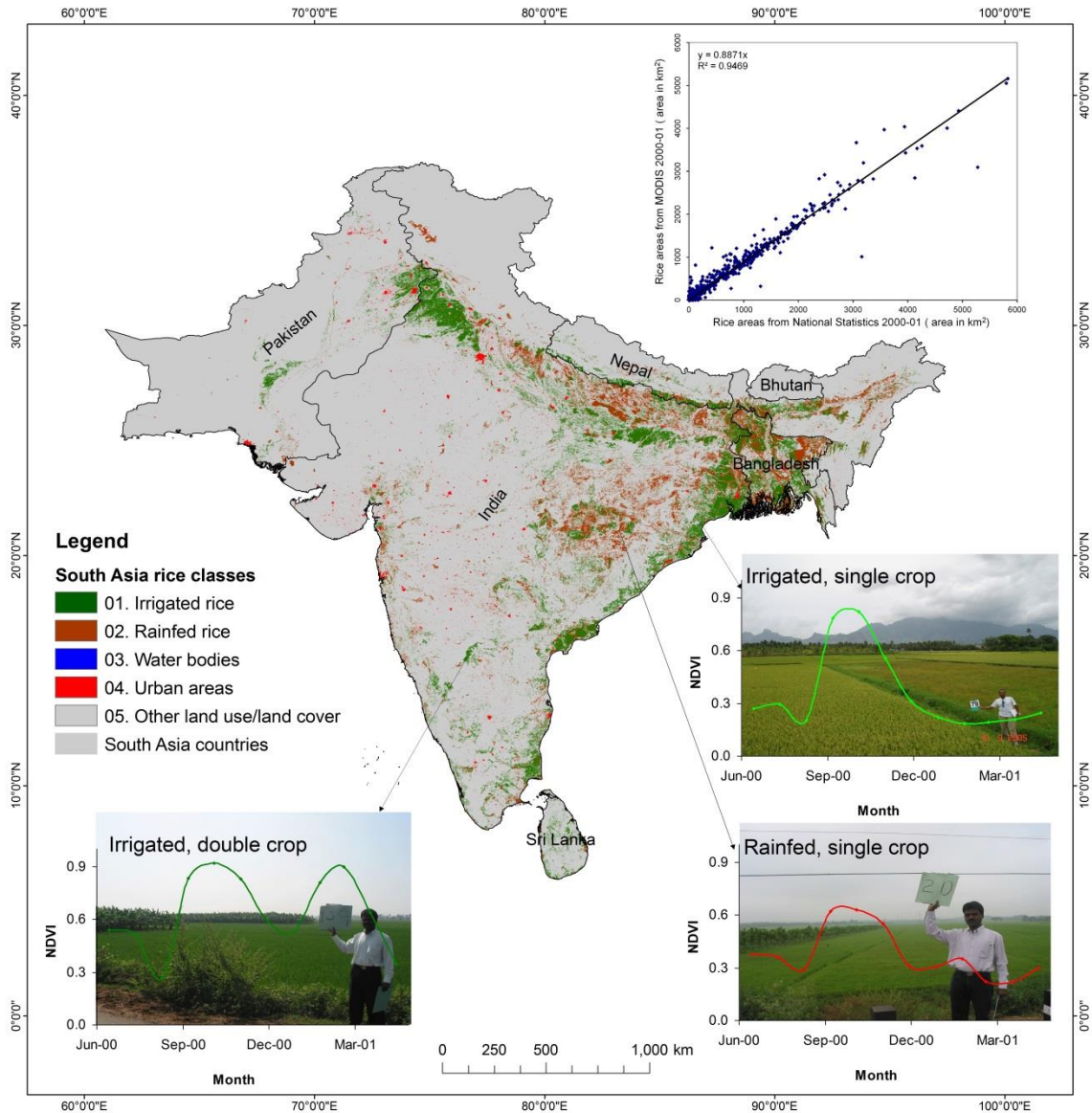


Figure 15. Rice map of south Asia produced using method illustrated in Figure 6. [Source: Gumma et al., 2011].

11.0 Conclusions

The chapter begins with providing an overview of the importance of global cropland products in food security analysis. It is obvious that only remote sensing from Earth Observing (EO) satellites provides consistent, repeated, high quality data for characterizing and mapping key cropland parameters for global food security analysis. Importance of definitions and class naming conventions in cropland mapping has been re-iterated. Typical EO systems and their spectral, spatial, temporal, and radiometric characteristics useful for cropland mapping have been highlighted. The chapter provides a review of various cropland mapping methods used at global, regional, and local levels. One of the methods of global cropland mapping using remote sensing

has been illustrated. The current state-of-art provides three key global cropland products derived from remote sensing, each produced by a different group. These products have been produced using: (a) time-series multi-sensor data and secondary data, (b) 250 m MODIS time-series data, and (c) Landsat 30 m. In addition, a MODIS 250 m time-series derived cropland classes from a land use\land cover product has also been used. These four products were synthesized, at nominal 1 km, to obtain a unified cropland mask of the world (named as global cropland extent version 1.0 or GCE V1.0; Figure 12a, 12b). It was obvious from these products that the uncertainty in location of croplands in any one given product is quite high. In other words, no single product maps croplands particularly well. So, a synthesis provides a good measure to see where some or all of these products agree and where they disagree. This actually becomes a starting point for next level of more detailed cropland mapping at 250 m and 30 m. The key cropland parameters identified to be derived from remote sensing are: (1) cropland extent\areas, (2) cropping intensities, (3) watering method (irrigated versus rainfed), (4) crop type, and (5) cropland change over time and space. From these primary products one can derive crop productivity and water productivity. Such products have great importance and relevance in global food security analysis.

12.0 Acknowledgements

The authors would like to thank NASA Making Earth Science Data Records for Use in Research Environments (MEaSUREs) solicitation for funding this research. Support by USGS Powell Center for a working group on global croplands is much appreciated. We thank the global food security support analysis data @ 30 m (GFSAD30) project team for inputs. Figure 1 and 2 were produced by Dr. Zhuoting Wu, Mendenhall Fellow, USGS. We thank her for it.

13.0 References

- Biggs, T., Thenkabail, P.S., Krishna, M., GangadharaRao, P., & Turrall, H. (2006). Vegetation phenology and irrigated area mapping using combined MODIS time-series, ground surveys, and agricultural census data in Krishna River Basin, India. *International Journal of Remote Sensing*, 27(19), 4245-4266.
- Bindraban, P. S., Bulte, E. H., & Conijn, S. G. (2009). Can large-scale biofuel production be sustained by 2020? *Agricultural Systems*, 101, 197-199.
- Biradar, C. M., P. S. Thenkabail, P. Noojipady, Y. Li, V. Dheeravath, H. Turrall, M. Velpuri, et al. 2009. "A Global Map of Rainfed Cropland Areas (GMRCA) at the End of Last Millennium Using Remote Sensing." *International Journal of Applied Earth Observation & Geoinformation* 11 (2): 114_129. doi:10.1016/j.jag.2008.11.002.
- Chander, G., Markham, B.L., and Helder,D.L. 2009. Summary of current radiometric calibration coefficients for Landsat MSS, TM, ETM+, and EO-1 ALI sensors, *Remote Sensing of Environment*, Volume 113, Issue 5, 15 May 2009, Pages 893-903, ISSN 0034-4257, <http://dx.doi.org/10.1016/j.rse.2009.01.007>
(<http://www.sciencedirect.com/science/article/pii/S0034425709000169>)
- Cohen, W. B., & Goward, S. N. (2004). Landsat's role in ecological applications of remote sensing. *BioScience*, 54, 535-545.
- Congalton, R. 2009. Accuracy and Error Analysis of Global and Local Maps: Lessons Learned and Future Considerations. IN: *Remote Sensing of Global Croplands for Food Security*. P. Thenkabail, J. Lyon, H. Turrall, and C. Biradar. (Editors). CRC/Taylor & Francis, Boca Raton, FL pp. 441-458.
- Congalton, R. and K. Green. 2009. *Assessing the Accuracy of Remotely Sensed Data: Principles and Practices*. 2nd Edition. CRC/Taylor & Francis, Boca Raton, FL 183p.
- Congalton, R. 1991. A review of assessing the accuracy of classifications of remotely sensed data. *Remote Sensing of Environment*. Vol. 37, pp. 35-46.
- Crist, E. P., & Cicone, R. C. (1984). Application of the tasseled cap concept to simulated Thematic Mapper data. *Photogrammetric Engineering and Remote Sensing*, 50, 343-352.
- DeFries, R., Hansen, M., Townsend, J. G. R., & Sohlberg, R. (1998). Global land cover classifications at 8 km resolution: the use of training data derived from Landsat imagery in decision tree classifiers. *International Journal of Remote Sensing*, 19, 3141-3168.
- Dheeravath, V., Thenkabail, P.S., Chandrakantha, G, Noojipady, P., Biradar, C.B., Turrall. H., Gumma, M.1, Reddy, G.P.O., Velpuri, M. 2010. Irrigated areas of India derived using MODIS 500m data for years 2001-2003. *ISPRS Journal of Photogrammetry and Remote Sensing*. <http://dx.doi.org/10.1016/j.isprsjprs.2009.08.004>. 65(1): 42-59.

EPW (2008). Food Security Endangered: Structural changes in global grain markets threaten India's food security. *Economic and Political Weekly*, 43, 5.

FAO (2009). Food outlook: Outlook Global Market Analysis. Rome: FAO.

Foley, J. A., Monfreda, C., Ramankutty, N., & Zaks, D. (2007). Our share of the planetary pie. *PNAS*, 104, 12585-12586.

Foley, J. A., DeFries, R, Asner, G.P., Barford, C., Bonan, G., Carpenter, S.R., Chapin, F.S., Coe, M.T., Daily, G.C., Gibbs, H.K., Helkowski, J.H., Holloway, T., Howard, E.A., Kucharik, C.J., et al., 2011. Solutions for a cultivated planet, *Nature*, 478(7369): 337-342.

Falkenmark, M., & Rockström, J. (2006). The New Blue and Green Water Paradigm: Breaking New Ground for Water Resources Planning and Management. *Journal of Water Resource Planning and Management*, 132, 1-15.

Friedl, M. A., McIver, D. K., Hodges, J. C. F., Zhang, X. Y., Muchoney, D., & Strahler, A. H. (2002). Global land cover mapping from MODIS: Algorithms and early results. *Remote Sensing of Environment*, 83, 287-302.

Friedl, M.A., Sulla-Menashe, D., Tan, B., Schneider, A., Ramankutty, N.S., and Huang, X.M. 2010. MODIS Collection 5 global land cover: Algorithm refinements and characterization of new datasets. *REMOTE SENSING OF ENVIRONMENT*, 114(1), 168-182.

Funk, C., & Brown, M. (2009). Declining global per capita agricultural production and warming oceans threaten food security. *Food Security*, DOI: 10.1007/s12571-009-0026-y.

Gibbs, H. K., Johnston, M., Foley, J. A., Holloway, T., Monfreda, C., Ramankutty, N., & Zaks, D. (2008). Carbon payback times for crop-based biofuel expansion in the tropics: the effects of changing yield and technology. *Environ. Res. Lett.*, 034001, doi: 10.1088/1748-9326/3/3/034001.

Goodchild, M. and S. Gopal (eds.) 1989. The Accuracy of Spatial Databases. Taylor and Francis. New York. 290 p.

Gordon, L. J., Finlayson, C. M., & Falkenmark, M. (2009). Managing water in agriculture for food production and other ecosystem services. *Agricultural Water Management*, 97, doi: DOI: 10.1016/j.agwat.2009.03.017.

Gumma, M.K., Nelson, A., Thenkabail, P.S., and Singh, A.N. 2011. "Mapping rice areas of South Asia using MODIS multi temporal data", *J. Appl. Remote Sens.* 5, 053547 (Sep 01, 2011); doi:10.1117/1.3619838.

Gutman, G., Byrnes, R., Masek, J., Covington, S., Justice, C., Franks, S., and Headley, R. 2008. Towards monitoring Land-cover and land-use changes at a global scale: the global land survey 2005. *Photogrammetric Engineering and Remote Sensing*. 74(1):6-10.

Goldewijk, K., A. Beusen, M. de Vos and G. van Drecht (2011). The HYDE 3.1 spatially explicit database of human induced land use change over the past 12,000 years, *Global Ecology and Biogeography* 20(1): 73-86.[DOI: 10.1111/j.1466-8238.2010.00587.x](https://doi.org/10.1111/j.1466-8238.2010.00587.x).

Hansen, M. C., DeFries, R. S., Townshend, J. R. G., Sohlberg, R., Dimiceli, C., & Carroll, M. (2002). Towards an operational MODIS continuous field of percent tree cover algorithm: examples using AVHRR and MODIS data. *Remote Sensing of Environment*. 83, 303-319.

Hossain, M., Janaiah, A., & Otsuka, K. (2005). Is the productivity impact of the Green Revolution in rice vanishing? *Economic and Political Weekly*, 5595-9600.

Jiang, Y. (2009). China's water scarcity. *Journal of Environmental Management*, 90, 3185-3196.

Khan, S., & Hanjra, M. A. (2008). Sustainable land and water management policies and practices: a pathway to environmental sustainability in large irrigation systems. *Land Degradation and Development*, 19, 469–487.

Kumar, M. D., & Singh, O. P. (2005). Virtual water in global food and water policy making: Is there a need for rethinking? *Water Resources Management*, 19, 759 - 789.

Kurz, B and Seelan, S. K. 2007. Use of Remote Sensing to Map Irrigated Agriculture in Areas Overlying the Ogallala Aquifer, United States. Book Chapter in Global Irrigated Areas. IWMI. Under Review.

Lal, R., & Pimentel, D. (2009). Biofuels from crop residues. *Soil and Tillage Research*, 93, 237-238.

Loveland, T. R., Reed, B. C., Brown, J. F., Ohlen, D. O., Zhu, Z., & Yang, L. (2000). Development of global land cover characteristics database and IGBP DISCover from 1 km AVHRR data. *International Journal of Remote Sensing*, 21, 1303-1330.

McIntyre, B. D. (2008). International assessment of agricultural knowledge, science and technology for development (IAASTD) : global report., *Includes bibliographical references and index*. ISBN 978-1-59726-538-6, Oxford, UK.

Masek, J. G., Huang, C., Wolfe, R., Cohen, W., Hall, F., Kutler, J., & Nelson, P. (2008). North American forest disturbance mapped from a decadal Landsat record. *Remote Sensing of Environment*, 112, 2914-2926.

Masek, J.G., E.F. Vermote, N. Saleous, R. Wolfe, F.G. Hall, Huemmrich, F.Gao, J.Kutler, and T.K.Lim, 2006, A Landsat surface reflectance data set for North America, 1990-2000, *Geoscience and Remote Sensing Letters*, 3, 68-72.

Monfreda, C., Patz, J. A., Prentice, I.C., Ramankutty, N., Snyder, P.K. Global consequences of land use Science. 2005 Jul 22; 309(5734):570-4.

Monfreda, C., N. Ramankutty, and J. A. Foley, 2008. Farming the planet: 2. Geographic distribution of crop areas, yields, physiological types, and net primary production in the year 2000, *Global Biogeochem. Cycles*, 22(1): GB1022.

Olofsson, P., Stehman, S.V., Woodcock, C.E., Sulla-Menasche, D., Sibley, A.M., Newell, J.D., Friedl, M.A., and Herold, M. 2011. A global land cover validation dataset, I: fundamental design principles. International Journal of Remote Sensing. In Review.

Ozdogan, M., & Gutman, G. (2008). A new methodology to map irrigated areas using multi-temporal MODIS and ancillary data: An application example in the continental US. *Remote Sensing of Environment*, 112, 3520-3537.

Ozdogan, M., & Woodcock, C. E. (2006). Resolution dependent errors in remote sensing of cultivated areas. *Remote Sensing of Environment*, 103, 203-217.

Ozdogan, M., and G. Gutman, 2008. A new methodology to map irrigated areas using multi-temporal MODIS and ancillary data: An application example in the continental US, *Remote Sensing of Environment*, 112(9): 3520-3537.

Pittman K., Hansen M.C., Becker-Reshef I., Potapov P.V., Justice C.O. Estimating Global Cropland Extent with Multi-year MODIS Data. *Remote Sensing*. 2010; 2(7):1844-1863.

Portmann, F., Siebert, S., & Döll, P. (2009). MIRCA2000 – Global monthly irrigated and rainfed crop areas around the year 2000: a new high-resolution data set for agricultural and hydrological modelling. *Global Biogeochemical Cycles*, 2008GB0003435.

Portmann, F., S. Siebert, and P. Döll, 2008. MIRCA2000 – Global monthly irrigated and rainfed crop areas around the year 2000: a new high-resolution data set for agricultural and hydrological modelling, *Global Biogeochemical Cycles*, GB0003435.

Ramankutty, N., Evan, A. T., Monfreda, C., & Foley, J. A. (2008). Farming the planet: 1. Geographic distribution of global agricultural lands in the year 2000. *Global Biogeochem. Cycles*, 22, doi:10.1029/2007GB002952.

Ramankutty, N., and J. A. Foley, 1998. Characterizing patterns of global land use: An analysis of global croplands data, *Global Biogeochemical Cycles*, 12(4): 667-685.

Rodell, M., Velicogna, I., Famiglietti, J. S., 2009, *Nature* 460, 999-1002, doi:10.1038/nature08238.

Searchinger, T., Heimlich, R., Houghton, R. A., Dong, F., Elobeid, A., Fabiosa, J., Tokgoz, S., Hayes, D., & Yu, T. H. (2008). Use of U.S. Croplands for Biofuels Increases Greenhouse Gases Through Emissions from Land-Use Change. *Science*, 319, 1238-1240.

Siebert, S., & Döll, P. (2009). Quantifying blue and green virtual water contents in global crop production as well as potential production losses without irrigation. *Journal of Hydrology*, doi:10.1016/j.jhydrol.2009.07.031.

Siebert, S., Hoogeveen, J., & Frenken, K. (2006). Irrigation in Africa, Europe and Latin America - Update of the Digital Global Map of Irrigation Areas to Version 4, *Frankfurt Hydrology Paper 05, 134 pp.* Institute of Physical Geography, University of Frankfurt, Frankfurt am Main, Germany and Rome, Italy.

Thenkabail, P.S., Mariotto, I., Gumma, M.K., Middleton, E.M., Landis, and D.R., Huemmrich, F.K., 2013. Selection of hyperspectral narrowbands (HNBS) and composition of hyperspectral twoband vegetation indices (HVIs) for biophysical characterization and discrimination of crop types using field reflectance and Hyperion/EO-1 data. *IEEE JOURNAL OF SELECTED TOPICS IN APPLIED EARTH OBSERVATIONS AND REMOTE SENSING*, Pp. 427-439, VOL. 6, NO. 2, APRIL 2013.doi: [10.1109/JSTARS.2013.2252601](https://doi.org/10.1109/JSTARS.2013.2252601)

Thenkabail P.S., Knox J.W., Ozdogan, M., Gumma, M.K., Congalton, R.G., Wu, Z., Milesi, C., Finkral, A., Marshall, M., Mariotto, I., You, S. Giri, C. and Nagler, P. 2012. Assessing future risks to agricultural productivity, water resources and food security: how can remote sensing help?. *Photogrammetric Engineering and Remote Sensing*, August 2012 Special Issue on Global Croplands: Highlight Article.

Thenkabail P.S., Wu Z. An Automated Cropland Classification Algorithm (ACCA) for Tajikistan by Combining Landsat, MODIS, and Secondary Data. *Remote Sensing*. 2012; 4(10):2890-2918.

Thenkabail, P.S., Hanjra, M.A., Dheeravath, V., Gumma, M. 2011. Book Chapter # 16: Global Croplands and Their Water Use Remote Sensing and Non-Remote Sensing Perspectives. In the Book entitled: “Advances in Environmental Remote Sensing: Sensors, Algorithms, and Applications”. Taylor and Francis Edited by Dr. Qihao Weng. Pp. 383-419.

Thenkabail P.S., Hanjra M.A., Dheeravath V., Gumma M. A. 2010. A Holistic View of Global Croplands and Their Water Use for Ensuring Global Food Security in the 21st Century through Advanced Remote Sensing and Non-remote Sensing Approaches. *Journal Remote Sensing*. 2(1):211-261. doi:10.3390/rs2010211. <http://www.mdpi.com/2072-4292/2/1/211>.

Thenkabail. P., Lyon, G.J., Turrel, H., and Biradar, C.M. 2009a. Book entitled: “Remote Sensing of Global Croplands for Food Security” (CRC Press- Taylor and Francis group, Boca Raton, London, New York. Pp. 556 (48 pages in color). Published in June, 2009.

Thenkabail, P.S., Biradar C.M., Noojipady, P., Dheeravath, V., Li, Y.J., Velpuri, M., Gumma, M., Reddy, G.P.O., Turrel, H., Cai, X. L., Vithanage, J., Schull, M., and Dutta, R. 2009b. Global irrigated area map (GIAM), derived from remote sensing, for the end of the last millennium. *International Journal of Remote Sensing*. 30(14): 3679-3733. July, 20, 2009.

Thenkabail, P. S., Lyon, G. J., Turrall, H., & Biradar, C. M. (2009c). *Remote Sensing of Global Croplands for Food Security*. Boca Raton, London, New York: CRC Press- Taylor and Francis Group, Published in June,.

Thenkabail, P.S., GangadharaRao, P., Biggs, T., Krishna, M., and Turrall, H., 2007a. Spectral Matching Techniques to Determine Historical Land use/Land cover (LULC) and Irrigated Areas using Time-series AVHRR Pathfinder Datasets in the Krishna River Basin, India. Photogrammetric Engineering and Remote Sensing. 73(9): 1029-1040. (Second Place Recipients of the 2008 John I. Davidson ASPRS President's Award for Practical papers).

Thenkabail, P.S., Biradar C.M., Noojipady, P., Cai, X.L., Dheeravath, V., Li, Y.J., Velpuri, M., Gumma, M., Pandey., S. 2007b. Sub-pixel irrigated area calculation methods. *Sensors Journal (special issue: Remote Sensing of Natural Resources and the Environment (Remote Sensing Sensors Edited by Assefa M. Melesse)*. 7:2519-2538. <http://www.mdpi.org/sensors/papers/s7112519.pdf>.

Thenkabail, P.S., Schull, M., Turrall, H. 2005. Ganges and Indus River Basin Land Use/Land Cover (LULC) and Irrigated Area Mapping using Continuous Streams of MODIS Data. *Remote Sensing of Environment*, 95(3): 317-341.

Thenkabail, P.S., Enclona, E.A., Ashton, M.S., Legg, C., Jean De Dieu, M., 2004. Hyperion, IKONOS, ALI, and ETM+ sensors in the study of African rainforests. *Remote Sensing of Environment*, 90:23-43.

Tillman, D., C. Balzer, J. Hill, and B. L. Befort, 2011. Global food demand and the sustainable intensification of agriculture, *Proceedings of the National Academy of Sciences of the United States of America, November 21, doi: 10.1073/pnas.1116437108*.

Turrall, H., Svendsen, M., & Faures, J. (2009). Investing in irrigation: Reviewing the past and looking to the future. *Agricultural Water Management*, doi:101.1016/j.agwt.2009.07.012.

UNDP (2012). Human Development Report 2012: Overcoming Barriers: Human Mobility and Development. New York: United Nations.

Velpuri, M., Thenkabail, P.S., Gumma, M.K., Biradar, C.B., Dheeravath, V., Noojipady, P., Yuanjie, L., 2009. Influence of Resolution or Scale in Irrigated Area Mapping and Area Estimations. *Photogrammetric Engineering and Remote Sensing (PE&RS)*. 75(12): December 2009 issue.

Vinnari, M., & Tapio, P. (2009). Future images of meat consumption in 2030. *Futures*, doi:10.1016/j.futures.2008.11.014.

Wada, Y., L. P. H. van Beek, and M. F. P. Bierkens (2012), Nonsustainable groundwater sustaining irrigation: A global assessment, *Water Resour. Res.*, 48, W00L06, doi:10.1029/2011WR010562.

Wardlow, B. D., & Egbert, S. L. (2008). Large-area crop mapping using time-series MODIS 250 m NDVI data: An assessment for the U.S. Central Great Plains. *Remote Sensing of Environment*, 112, 1096-1116.

Wardlow, B. D., Egbert, S. L., & Kastens, J. H. (2007). Analysis of time-series MODIS 250 m vegetation index data for crop classification in the U.S. Central Great Plains. *Remote Sensing of Environment*, 108, 290-310.

Wardlow, B. D., Kastens, J. H., & Egbert, S. L. (2006). Using USDA crop progress data for the evaluation of greenup onset date calculated from MODIS 250-meter data. *Photogrammetric Engineering and Remote Sensing*, 72, 1225-1234.

Wu, Z., Thenkabail, P.S., Zakzeski, A., Mueller, R., Melton, F., Rosevelt, C., Dwyer, J., Johnson, J., Verdin, J. P., 2014a. Seasonal cultivated and fallow cropland mapping using modis-based automated cropland classification algorithm. *J. Appl. Remote Sens.* 0001;8(1):083685. doi:10.1117/1.JRS.8.083685.

Wu, Z., Thenkabail, P.S., and Verdin, J. 2014b. An automated cropland classification algorithm (ACCA) using Landsat and MODIS data combination for California. *Photogrammetric Engineering and Remote Sensing*. Vol. 80(1): 81-90.

Yu, L., Wang, J., Clinton, N., Xin, Q., Zhong, L., Chen, Y., and Gong, P. 2013. International Journal of Digital Earth. FROM-GC: 30 m global cropland extent derived through multisource data integration, *International Journal of Digital Earth* ,DOI:10.1080/17538947.2013.822574.